Title

Dietary fiber monosaccharide content alters gut microbiome composition and fermentation.

Journal

Applied and Environmental Microbiology, 90(8)

Authors

Jensen, Nick

Maldonado-Gomez, Maria

Krishnakumar, Nithya

et al.

Publication Date

2024-08-21

DOI

10.1128/aem.00964-24

Peer reviewed

AMERICAN SOCIETY FOR MICROBIOLOGY | Applied and Environmental Microbiology

Food Microbiology | Full-Length Text

Dietary fiber monosaccharide content alters gut microbiome composition and fermentation

Nick Jensen,[1,2] Maria Maldonado-Gomez,[1,2] Nithya Krishnakumar,[1,2] Cheng-Yu Weng,[3] Juan Castillo,[3] Dale Razi,[2] Karen Kalanetra,[1,2] J. Bruce German,[1,2] Carlito B. Lebrilla,[2,3] David A. Mills,[1,2] Diana H. Taft[4]

AUTHOR AFFILIATIONS See affiliation list on p. 19.

ABSTRACT Members of the mammalian gut microbiota metabolize diverse complex carbohydrates that are not digested by the host, which are collectively labeled "dietary fiber." While the enzymes and transporters that each strain uses to establish a nutrient niche in the gut are often exquisitely specific, the relationship between carbohydrate structure and microbial ecology is imperfectly understood. The present study takes advantage of recent advances in complex carbohydrate structure determination to test the effects of fiber monosaccharide composition on microbial fermentation. Fifty-five fibers with varied monosaccharide composition were fermented by a pooled feline fecal inoculum in a modified MiniBioReactor array system over a period of 72 hours. The content of the monosaccharides glucose and xylose was significantly associated with the reduction of pH during fermentation, which was also predictable from the concentrations of the short-chain fatty acids lactic acid, propionic acid, and the signaling molecule indole-3-acetic acid. Microbiome diversity and composition were also predictable from monosaccharide content and SCFA concentration. In particular, the concentrations of lactic acid and propionic acid correlated with final alpha diversity and were significantly associated with the relative abundance of several of the genera, including *Lactobacillus* and *Dubosiella*. Our results suggest that monosaccharide composition offers a generalizable method to compare any dietary fiber of interest and uncover links between diet, gut microbiota, and metabolite production.

IMPORTANCE The survival of a microbial species in the gut depends on the availability of the nutrients necessary for that species to survive. Carbohydrates in the form of non-host digestible fiber are of particular importance, and the set of genes possessed by each species for carbohydrate consumption can vary considerably. Here, differences in the monosaccharides that are the building blocks of fiber are considered for their impact on both the survival of different species of microbes and on the levels of microbial fermentation products produced. This work demonstrates that foods with similar monosaccharide content will have consistent effects on the survival of microbial species and on the production of microbial fermentation products.

KEYWORDS fiber, gut microbiome, prebiotic, fermentation, anaerobes

The human diet primarily comprises fats, proteins, and carbohydrates, with the latter macronutrient contributing the majority of calories in most societies (1). Besides starches and sugars that are readily digested by mammals, dietary carbohydrate sources include various types of indigestible fiber (2). Though molecules such as cellulose are relatively inert, many other types of dietary fiber act as "microbiota-accessible carbohydrates" (MACs), which serve as substrates for metabolism by the gut microbiota (3). These carbohydrates are fermented into bioactive end products such as short-chain fatty acids (SCFAs) that may influence host physiology by altering the pH of the intestinal lumen,

Editor Danilo Ercolini, Universita degli Studi di Napoli Federico II, Portici, Italy

Address correspondence to Diana H. Taft, dianataft@ufl.edu, or David A. Mills, damills@ucdavis.edu.

Nick Jensen and Maria Maldonado-Gomez contributed equally to this article. Author order was based on experimental, computational, and manuscript writing labor.

D.A.M., J.B.G., and C.B.L. are cofounders of Infinant Health, a probiotic company, and One.Bio, a company advancing novel bioactive glycans. None of these companies had any role in the conceptualization, design, analysis, or preparation of the manuscript.

See the funding table on p. 20.

Received 14 May 2024
Accepted 18 June 2024
Published 15 July 2024

contributing to energy balance, and regulating transcription in a variety of metabolic and immune cells by signaling via the receptors Ffar2 and Ffar3 (1). While many dietary plants, including beets, alfalfa, oats, corn, and soy, are recognized as potential sources of MACs (4), the specific chemical structures within these carbohydrates that facilitate microbial metabolism are often unknown.

Knowledge of diet-derived MAC structure is important because distinct carbohydrates are known to influence the composition and function of the mammalian gut microbiota. Many strains of gut bacteria are predicted to encode specific carbohydrate-binding molecules alongside hundreds of carbohydrate-active enzymes that may recognize specific linkages (5). These enzymes' mechanisms of action may depend on glycan complexity (6) and can entail many coordinated steps (2, 3). In some cases, the metabolism of a carbohydrate may be performed by multiple species (7, 8). Gut bacterial genera such as *Bacteroides* and *Prevotella* express diverse glycoside hydrolases, polysaccharide lyases, and carbohydrate esterases, enzymes that are known or predicted by proteomics to break down distinct polysaccharides, such as xylans, pectin, and arabinogalactans (9, 10). The expression of carbohydrate-active enzymes varies extensively within genera and species (11); for example, the species *Bifidobacterium longum* includes the infant-associated *B. longum* subsp. *infantis*, which encodes a gene cluster for metabolizing human milk oligosaccharides (HMOs) (12), as well as adult-associated strains of *B. longum* subsp. *longum* that specializes in plant oligosaccharide metabolism (13). Certain microbes can be enriched by targeted provision of specific carbohydrate structures, such as acetylated galactoglucomannans (14, 15) and arabinooligosaccharides (4). Species of the genus *Bacteroides* are known to compete for multiple glycans, such as arabinan (16), but may coexist due to differences in physicochemical complexity (17) or substrate prioritization (18), illustrating the intimate relationship between carbohydrate structure and microbial ecology. These bacterial-fiber relationships can hold true across host species, which is why humans, canines, and felines have generally similar gut microbial phylogeny and functional capacity (19). Because cats have reduced digestive enzyme capacity (20), cats make a good model organism to test for associations between fiber structure and microbiome response as a greater percentage of the carbohydrate in food might be available to the gut microbes.

Despite increasing recognition of carbohydrate structure as a determinant of gut microbial dynamics, the carbohydrate content of many foods remains poorly characterized, and the mechanisms of gut microbiome metabolism are only partially elucidated. Starchy plants are staple foods in many human diets, but dietary starch encompasses both soluble amylopectin that is readily digested and five types of resistant starch, which may be microbiota-accessible (21). MACs from different food sources may differ in their discrete structure in terms of monosaccharide content, chemical linkages, isomerism, chain length, and modifications such as methylation and sulfation, all of which may differentially affect their degradation by specific gut microbial enzymes (22, 23). Fermentation by the gut microbiota can be impacted by relatively fine differences in MAC structure, such as arabinoxylans from different kinds of wheat bran (24, 25), the degree of polymerization of oligosaccharides derived from sugar beet pectin (26), and the linkages found in glucans (27). However, due to the complex physicochemical properties of food carbohydrates (28) and the analytical difficulties of isolating and analyzing glycans (29), the exact composition of most diet-derived MACs is unknown.

Recently, novel approaches based on ultra-performance liquid chromatography and triple-quadrupole mass spectrometry (UPLC-QqQ-MS) are able to address the challenges of studying the fine structure of complex carbohydrates (30, 31). These techniques can reveal, in high throughput, the monosaccharide composition of any carbohydrate of interest (30), data that have been collected for more than 800 foods in the "Davis Food Glycopedia" (31). Precise monosaccharide composition offers a simple, generalizable means of comparison between numerous dietary fibers, permitting the analysis of how dietary carbohydrate structure affects gut microbiome function at an unprecedented scale.

The present study aimed to determine if differences in fiber monosaccharide content influenced the composition and metabolic function of a model gut microbiota. Data on the monosaccharide composition of foods, portions of which have been published in the Davis Food Glycopedia, guided the selection of 55 qualitatively diverse fibers with varied monosaccharide content. In order to model mammalian microbiome function *in vitro*, each fiber was fermented over 72 hours in a bioreactor. 16S rRNA gene sequencing was performed in order to identify changes in the microbiome in tandem with the quantification of pH and short-chain fatty acids.

MATERIALS AND METHODS

Monosaccharide composition

Fiber monosaccharide composition data were obtained with UPLC-QqQ-MS, as previously described (30).

Food processing

Foods (Table S1) were processed to model mastication prior to digestion. All foods were purchased from local grocers and stored at 4°C prior to processing in the Food Instruction Lab at the Robert Mondavi Institute for Wine and Food Science. Foods with low water content, such as fried seaweed, were ground into a powder using a Vitamix. Foods with high water content, such as fresh apples, were diced and ground into a slurry using a Vitamix. In some cases, water was added to achieve a homogeneous slurry. The addition of water was recorded and accounted for in the *in vitro* digestion calculations. After processing, foods were stored in Quart Ziplock Bags at −20°C until digestion.

In vitro digestion of foods

The *in vitro* protocol to mimic cat digestion was modeled on the INFOGEST protocol, a previously validated human *in vitro* digestion system (5). The following changes were made to adapt the protocol to the cat digestive system. Simulated salivary fluids (SSFs), simulated gastric fluids (SGFs), and simulated intestinal fluids (SIFs) were adapted from the INFOGEST protocol to match the minerals found in the cat saliva, gastric fluid, and intestinal fluid, respectively. In cases where a range of mineral concentrations is common, the average between the minimum and maximum reported values was used. Table S2 details the range of mineral concentrations reported as well as the reference material. Table S3 details the final composition of 1.25X SSF, SGF, and SIF used.

In the oral phase, salivary alpha-amylase was removed, given that cats do not secrete the enzyme, and pH was adjusted to 7.5 based on the average pH of cat saliva (32). The food slurry was mixed with 1.25× SSF, pH of the mixture was adjusted to 7.5, and the final volume was adjusted using deionized (DI) water for a final ratio of 1:1 food slurry and SSF. The oral bolus was incubated at 37°C with agitation for 2 min. To simulate gastric digestion, the oral bolus was mixed with 1.25× SGF, 2,000 U/mL pepsin (Sigma P6887), and adjusted to pH 2.5 using 6 M HCl (33). DI water was added for a final ratio of 1:1 oral bolus and SGF. The gastric fluid was incubated at 37°C with agitation for 3 hours. While gastric emptying time varies by the individual cat and by the type of food eaten, 3 hours was chosen as a standard based on the average gastric emptying time for dry cat food (34). To simulate intestinal digestion, the gastric chyme was mixed with 1.25× SIF, pancreatin based on trypsin activity at 100 TAME Units/mL (Sigma P7545) (35), 11.5 U/mL amylase (Sigma A6814), and 5 mg/mL bovine bile (Sigma B3883) (32). The contribution of amylase in cats is very low, given that their diets are rich in protein. However, there is some evidence that amylase secretion in the pancreas increases after prolonged feeding of a high-carbohydrate diet. The amylase concentration was chosen based on the average amylase secretion from four healthy adult cats fed a diet containing potato starch for 3 weeks (36). The pH of the mixture was adjusted to 6.0 using 1 M NaOH (33). The intestinal slurry was incubated at 37°C with agitation for 2.5 hours, a time chosen

based on the average intestinal emptying time of the cat (32). After incubation, the intestinal slurry was immediately frozen at −20°C to halt enzymatic activity and stored until further use.

Dialysis and anthrone assays

Intestinal slurries were dialyzed to remove monosaccharides and excess salts using Biotech Cellulose Ester Dialysis Membranes (31 mm flat width, 100–500 D molecular weight cut-off, Catalog No. 888–10723, Repligen, Waltham, MA) Dialysis membranes were cut to a length of 400–550 mm and stored in 1% (vol/vol) formaldehyde (refreshed every 2–3 rounds of dialysis). Prior to each use, dialysis membranes were hydrated and rinsed with distilled water. Approximately 110–220 mL of thawed intestinal slurries were pipetted into each dialysis membrane. The filled dialysis membranes were submerged in a 30 L tub containing 22.5 L of distilled water. No more than 14 dialysis tubes (representing ~350 mL of intestinal slurry) were placed into the same dialysis container. Foods were often dialyzed together, and groupings were chosen to avoid intestinal slurries with either a high volume, high monosaccharide content, or high salt content being dialyzed together. The dialysis container was stored at 2°C for the duration of dialysis. Twice per day, the water was exchanged with fresh distilled water. After 96 hours, the dialyzed intestinal slurries were harvested from the dialysis membranes, placed into Gallon Ziploc Freezer Bags, and stored at −20°C until freeze drying.

Dialyzed intestinal slurries were lyophilized to remove water content using The Scientific Freeze Dryer (4-tray dryer, Medium, Harvest Right, North Salt Lake, UT). The slurries were thawed in a room temperature water bath, and then poured into even layers onto freeze dryer trays. Large volumes (>1.5 L) of dialyzed intestinal slurry were freeze dried in multiple batches and homogenized. Freeze drying conditions were −30°F (−34°C) for 4 hours, vacuum off; 35°F (1.7°C) for 3 hours, vacuum on; 80°F (26.7°C) for 12 hours, vacuum on; 120°F (48.9°C) for 5 hours, vacuum on. The material was then held at 120°F (48.9°C) with the vacuum on until it was retrieved from the machine. The lyophilized powder was then homogenized in a coffee grinder and stored in 50 mL conical tubes kept at −20°C. All lyophilized powders were stored in sealed secondary containers with desiccant prior to anthrone assays.

Anthrone assays were performed to determine the total fiber content of the lyophilized powders. A serial dilution of fibers and amylopectin standards were prepared at 0.75 mg/mL, 0.6 mg/mL, 0.5 mg/mL, 0.4 mg/mL, 0.25 mg/mL, and 0.1 mg/mL. Seventy microliter of serially diluted fibers or amylopectin was combined with 140 µL of 2 mg/mL anthrone in 6 M sulfuric acid in 0.5 mL strip tubes. Reactions were run in duplicate. The strip tubes were centrifuged and run in a Thermocycler at 90°C for 11 min followed by 20°C for 8 min. Samples were transferred to 96-well plates, and fluorescence data were obtained with a plate reader. The total fiber content of the lyophilized powder was then calculated.

Batch fermentation media

To make base media, in 80% total volume of DI water, the following components were dissolved: 0.05 g/L bile salts, 1 g/L casitone (hydrolyzed casein), 0.67 g/L proteose peptone no. 3, 4.83 g/L NaCl, 5 g/L K_2HPO_4, 3.19 g/L KH_2PO_4, 1.93 g/L $NaHCO_3$, 2.33 g/L Na_2CO_3, 9.76 g/L 2-(N-morpholino)ethanesulfonic acid, 0.50 g/L cysteine-HCl, 0.60 mL/L of 0.1% resazurin in water, 1 mL/L of 500 mg/mL $MgSO_4*7H_2O$ in water, 10 mL/L hemin solution (1 mg/mL in 0.02M NaOH), 2 mL/L Tween 80, 1.80 mL $FeSO_4*7H_2O$ solution (2.78 mg/mL in water and 6 M HCl dropwise to dissolve), 2 mL/L mineral solution (0.5 g/L EDTA, 0.2 g/L $FeSO_4*7H_2O$, 0.01 g/L $ZnSO_4*7H_2O$, 0.003 g/L $MnCl_2*7H_2O$, 0.03 g/L boric acid, 0.02 g/L $CoCl_2*6H_2O$, 0.001 g/L $CuCl_2*2H_2O$, 0.002 g/L $NiCl_2*6H_2O$, 0.003 g/L $NaMOO_4*4H_2O$ dissolved in water), 5.6 mL/L vitamin solution [0.25 g/L menadione, 0.5 g/L biotin, 0.5 g/L pantothenate, 2.5 g/L nicotinamide (niacin), 0.125 g/L vitamin B12, 1 g/L thiamine, and 1.25 g/L p-aminobenzoic acid dissolved in 63% ethanol], and 1 mL of 20 mg/mL $CaCl_2*2H_2O$ in water. This solution was filter-sterilized (0.2 µm pore-size),

covered with foil, and placed immediately under anaerobic conditions for 48 hours before use to remove oxygen. Media was made fresh before each experiment.

Batch fermentations of fibers

Batch fecal fermentations were conducted in triplicate with 55 unique fibers, divided into nine experiments. In addition to the fibers, one no carbohydrate control was included in each experiment. Fermentations were conducted in an anaerobic chamber using a MiniBioReactor Array system (37, 38) in batch mode. Feline fecal samples (provided by Mars, Inc., McLean, VA) were used to inoculate fermentations. Because the fecal microbiome of cats has been found to cluster by both subject and the date of sampling within subjects (39), a single inoculum for all fermentations was created by pooling 10 fecal samples with distinct microbial communities. Samples to be pooled were selected based on the microbial communities' dissimilarities between available samples. Dissimilarities were calculated using 16S rRNA gene sequencing data of each individual available fecal sample and Bray Curtis index (data not shown). The 10 most distinct samples were pulled to maximize microbial diversity and functional genetic richness. The fecal inoculum for each fermentation was placed in the anaerobic chamber, and 25% m/v fecal slurry was made using previously reduced 1× PBS. Slurries were homogenized by vortexing for 5 min and centrifuged at 200 g for 5 min to separate large particles. The supernatant was mixed with fermentation media in a 20:80 ratio and incubated for 72 hours with constant stirring, under anaerobic conditions. Experimental fermentation media contained 1% m/v of the fiber of interest. No carbohydrate was added to control fermentations. One thousand five hundred microliters of samples was collected and split into 0.5 mL and 1 mL aliquots after 0, 24, 48, and 72 hours of batch fermentation. From the 0.5 mL sample, pH was immediately measured as samples were retrieved, and all samples were then preserved at −80°C prior to subsequent analyses (quantification of short-chain fatty acids and 16S rRNA gene sequencing).

Quantification of SCFAs

Sample preparation and derivatization

The SCFA quantification workflow was adapted from a previous publication (40). A pooled standard solution comprising 19 carboxylic acid metabolites was formulated in methanol (MeOH) and serially diluted to concentrations ranging from 0.001 µg/mL to 500 µg/mL, depending on the specific analytes. The batch fermentation supernatants were thawed and centrifuged at 13,500 rpm for 5 min. The supernatant was then collected and diluted 25-fold in MeOH. An internal standard mixture containing 100 µg/mL of d4-acetic acid, 50 µg/mL of d2-indolepropionic acid, and 10 µg/mL of 2-ethylbutyric acid was spiked into all standards and samples at the ratio of 1:10 (vol/vol). Two hundred microliter of acetonitrile (ACN) and 100 µL of derivatization reagent containing 20 mM triphenylphosphine, 20 mM dipyridyl disulfide, and 20 mM 2-picolylamine in ACN was plated in a 1 mL 96-well plate in advance. Ten microliter aliquots of standard or sample was dispensed into each well of the plate, which was then sealed and incubated at 60°C for 10 min. The entirety of the procedure was conducted within a 4°C cold room to minimize the evaporation of volatile analytes. Upon completion of the reaction, the derivatized samples were subjected to drying in a miVac concentrator. The dried samples were then reconstituted with 50% MeOH prior to instrumental analysis. Data are reported in micrograms per milliliter (µg/mL). The analysis was limited to the following metabolites: acetic acid, propionic acid, butyric acid, lactic acid, indole-3-propionic acid (I3P), indole-3-butyric acid (I3B), and indole-3-acetic acid (I3A).

Liquid chromatograpy with tandem mass spectrometry (LC-MS/MS) analysis

Derivatized analytes were analyzed on an Agilent 6495B QqQ MS coupled to an Agilent 1290 Infinity II UHPLC, as previously described in greater detail (40). Separation was performed on an Agilent Poroshell 120 EC-C18 column (2.1 mm × 100 mm, 1.9 µm

particle size). Aqueous mobile phase A consisted of 100% nano-pure water. Organic mobile phase B consisted of a 1:1 (vol/vol) ACN/isopropyl alcohol mixture. The following binary gradient was used: 0.00–1.00 min, 5.00% B; 1.00–10.00 min, 5.00%–20.00% B; 10.00–11.00 min, 20.00% B; 11.00–15.00 min, 20.00%–60.00% B; 15.00–16.00 min, 60.00%–5.00% B. One microliter of sample was injected in each run. The mobile phase flow rate was 0.45 mL/min, and the column temperature was set to 45°C. The Jet Stream Technology (AJS) electrospray ionization ion source was employed in positive ion mode, with the following parameters: capillary voltage = 1,800 V, nozzle voltage = 1,500 V, gas temperature = 240°C, gas flow = 20 L/min, nebulizer pressure = 25 psi, sheath gas temperature = 300°C, and sheath gas flow = 9 L/min. Mass spectrometry data were acquired using dynamic multiple reaction monitoring mode.

DNA extraction, library prep, and 16S rRNA gene sequencing

Genomic DNA was extracted using Zymobiomics 96 MagBead DNA Kit (Zymo Research, Irvine, CA) with a Kingfisher Flex automated extraction instrument (Thermo Fisher Scientific, Waltham, MA). As previously described (41), the V4 region of the 16S rRNA gene was amplified in triplicate with barcoded PCR primers F515 and R806. Amplicons were verified by gel electrophoresis, combined and purified, and sent to the UC Davis Genome Center for library preparation and high throughput 250 paired-end sequencing using an Illumina MiSeq. The sequencing run was performed in two batches. A ZymoBIOMICS mock community was used as a positive control.

Bioinformatics

Raw sequencing data were demultiplexed with Sabre (42). Demultiplexed data were imported into QIIME2-2021.2 (43), where data were quality filtered, and reads were processed with DADA2 (44). After filtering, taxonomy was assigned to reads using a pre-generated naïve Bayes classifier trained on Silva 138 99% operational taxonomic units (OTUs) from the 515F/806R region of sequences (45–47), accessed via QIIME2-2021.2 (43). Reads mapped to the microbial orders Caldalkalibacillales, Rhizobiales, Sphingomonadales, Micrococcales, and Bacilliales were present in three negative controls on one DNA extraction plate; therefore, contamination was suspected. Contaminant sequences were statistically identified using decontam (v. 1.1.1) (48) with default settings and pruned from the data set using phyloseq (v. 1.34.0) (49), resulting in the removal of 1/1,854 taxa from batch 1 samples and 21/1,854 taxa from batch 2 samples.

Statistical methods

All statistical analyses were completed in R 4.2.0 statistical software (50) and QIIME2-2021.2 (43).

Density-based spatial clustering of applications with noise

Fibers were clustered based on unadjusted monosaccharide composition using the clustering algorithm DBSCAN (density-based spatial clustering of applications with noise), as implemented in R with the package dbscan (v. 1.1–10) (51). Because the data were high-dimensional and little domain knowledge exists for choosing an appropriate value of the ε parameter (52), hierarchical DBSCAN with simplified hierarchy extraction was performed with a value of minPts = 3.

Data filtering and standardization

Multicollinearity among monosaccharides was identified with caret (v. 6.0–92) with a cutoff of absolute correlation >0.70, which resulted in the monosaccharides fucose, GlcNac, GalNac, and arabinose being filtered from the data set and excluded from subsequent analyses. Linear dependencies and variables with near-zero variance were

not detected in monosaccharide data. Values of the retained monosaccharides were multiplied by the mass of fiber (mg) used in fermentations to accurately reflect the amount of carbohydrate present in each fermentation. In order to standardize monosaccharide data across fibers, filtered and corrected monosaccharide values were scaled from 0 to 1 by subtracting the minimum value of each monosaccharide and dividing the result by the difference between the minimum and maximum values for that monosaccharide. The same parameters were used to identify multicollinearity among SCFAs with caret, with the exception that a cutoff of >0.50 absolute correlation was applied, resulting in the exclusion of acetic acid, butyric acid, and indole-3-propionic acid from subsequent analyses. The remaining SCFAs (propionic acid, lactic acid, indole-3-butyric acid, and indole-3-acetic acid) were also scaled from 0 to 1 using the same scaling function as for monosaccharides.

Hierarchical clustering

Fibers were grouped by hierarchical clustering based on filtered, corrected, and scaled monosaccharide composition data. A distance matrix based on Euclidean distance between monosaccharide values was calculated. Hierarchical clustering was performed with the hclust function in the base R package using both complete and average linkage, and Dunn's index was calculated for different values of *k* to find its maximum value. The heatmap function was used to plot a heatmap of monosaccharide hierarchical clustering results based on complete linkage. Similarly, filtered and scaled SCFA data were grouped with hierarchical clustering and visualized with a heatmap using the same parameters as for monosaccharides; however, average values of SCFA concentrations were used due to the variation between samples.

Modeling with final pH as outcome

To assess the effect of monosaccharide composition on final pH, we used a generalized linear model as implemented in the base package of R. Only monosaccharides found to have an absolute correlation below 0.70 with caret were eligible for inclusion. Purposeful selection was used to select the variables to include in the final model. Log or Box–Cox transformations were applied to monosaccharide data that deviated from normality, as assessed with the Shapiro–Wilk test. If a monosaccharide had at least one zero value for food, a pseudocount was added prior to transformation.

Alpha diversity

After excluding statistically identified contaminants, samples were rarefied without replacement to a depth of 2,509 reads using the vegan package (v. 2.5.7) (53), which retained 1,881,750 features (15.56% of features) in 750 samples (92.59% of samples). Rarefied data were used to calculate alpha diversity with the Shannon index using the vegan package [vegan package (v. 2.6–2) (53)] with default settings. To assess the effect of monosaccharide composition on longitudinal alpha diversity, a linear mixed effects (LMEs) model was implemented with the lmer function in the package lmerTest (v. 3.1.3) (54). Bioreactor ID was used as the grouping variable. Alpha diversity was observed to vary at baseline, so baseline alpha diversity was considered as a variable in the model. Day, baseline alpha diversity, and each monosaccharide were considered as fixed effects. Bioreactor ID was considered as a random effect since it was expected that the baseline values and rate of change would differ between fermentations. Log or Box–Cox transformations were considered for variables that deviated from normality, as assessed with the Shapiro–Wilk test. However, these transformations did not improve the normality of monosaccharide data across the entire time course of fermentation, so they were ultimately not applied. A modified form of purposeful selection was used to select the variables to include in the final model. Separate models were evaluated for each monosaccharide and baseline alpha diversity; each of these models included day as a fixed effect and fermenter as a grouping variable. Restricted maximum likelihood

was set to FALSE since the models compared different fixed effects. Variables that were significantly associated with alpha diversity were then assessed in a combined model, and the assumptions of linearity, homogeneity of variance, and normality of residuals were tested. Although a significant result was obtained in the analysis of variance of the squared residuals for bioreactor ID (*P*-value = 5.374e-12 by Levene's test), the histogram of the residuals did not appear bimodal. Therefore, since a q-q plot showed relatively linear residuals apart from extrema, the results of Levene's test were disregarded, and other variables were added back into the model by purposeful selection. A confidence interval was calculated using the confint function in the base R package.

Regression trees

Regression trees were constructed with the rpart package (v. 4.1.16). For final pH, data were divided into training (131 samples, mean final pH = 6.12) and test (30 samples, mean final pH = 6.15) sets, and the tree was pruned at a complexity parameter of 0.060944. For final alpha diversity, data were divided into training (118 samples, mean final alpha diversity = 2.75) and test (40 samples, mean final alpha diversity = 2.77) sets, and the tree was pruned at a complexity parameter of 0.031896. The performance of trees on test data was summarized with caret.

Beta diversity

Rarefied data were used to analyze beta diversity (between-sample diversity) because read depth varied more than 10-fold between samples. A distance matrix based on Bray–Curtis distance between samples was calculated based on decontaminated 16S rRNA gene sequencing data with the function vegdist in the vegan package (v. 2.5.7) (53). Bray–Curtis distance was selected as a distance metric instead of weighted or unweighted Unifrac (55) due to the presence of unassigned reads that became outliers if phylogeny was taken into account. Sequencing data were subsetted by day with phyloseq (v. 1.34.0) (49). Differences in beta diversity by monosaccharide composition were tested with permutational analysis of variance (PERMANOVA), as implemented by the adonis2 command in vegan, which can accommodate continuous variables. A backward elimination approach was used to select the final variables for each day's model. Ordination with nonmetric multidimensional scaling (NMDS) was performed with the metaMDS command in vegan to visualize day 3 beta diversity data. Ordinations with points colored using a gradient based on fiber monosaccharide content and pH were created with the plotfunctions package (v. 1.4).

Differential abundance

Differential abundance based on monosaccharide composition and SCFA concentration was tested with Analysis of Composition of Microbiomes (ANCOM) (56) in QIIME2-2021.2. Because ANCOM requires discrete variables, monosaccharide composition and SCFA concentration values were classified into tertiles with the functions quantile and cut in the base R package. Tertiles were chosen over quartiles or quintiles due to the relatively large number of very small values in many variables. 16S rRNA sequencing data were filtered to exclude samples prior to day 3. Taxonomy was collapsed to the genus level. Pseudocounts were added due to the presence of zeros in microbiome data. ANCOM was run separately for each monosaccharide and SCFA tertile.

RESULTS

In order to test the effects of fiber monosaccharide composition on the outcome of gut microbial fermentation, dietary fibers from 55 unique foods with known monosaccharide composition were chosen (31). These food fibers were selected to represent a diverse range of dietary fruits, vegetables, and starches common in human diets. The relatively large number of fibers analyzed presented a challenge for robust cross-fiber comparisons. We, therefore, sought to reduce the number of dimensions with clustering

analysis. Results of clustering with hierarchical DBSCAN (Fig. S1) identified few clusters based on monosaccharide composition with unbalanced membership and a high degree of noise. Moreover, hierarchical clustering identified a large number of clusters (data not shown), with Dunn's Index maximized at $k = 43$. Therefore, instead of grouping fibers into clusters, monosaccharide composition was compared directly across fibers.

The monosaccharide composition of each fiber was documented in terms of the content of glucose, galactose, fructose, xylose, arabinose, fucose, rhamnose, glucuronic acid (GlcA), galacturonic acid (GalA), *N*-acetylglucosamine (GlcNac), *N*-acetylgalactosamine (GalNac), mannose, allose, and ribose (Table S1). Some sugars, such as ribose and fucose, were relatively scarce in most food fibers in this data set, while others, such as glucose, were present in many fibers. Some monosaccharides were found to exhibit multicollinearity, and the sugars fucose, GlcNac, GalNac, and arabinose (absolute correlation > 0.50) were filtered from the data set. While the data for some monosaccharides were zero-inflated, no monosaccharides were found to have near-zero variance (data not shown).

In order to determine how fiber monosaccharide composition affected fermentation, each fiber was batch fermented in triplicate for a time course of 72 hours in the presence of a pooled feline fecal inoculum. Samples included in the inoculum were chosen to maximize the taxonomic richness and the functional capability to utilize different fiber substrates (see details in the Materials and Methods section). Prior to fermentation, foods were processed to model mastication and exposed to simulated digestive fluids *in vitro* to mimic feline digestion, after which free monosaccharides were removed with dialysis, and the total fiber content was measured with anthrone assays (see Materials and Methods) to create a standard concentration of 1% m/v of the fiber of interest in each fermentation. For most fibers, pH decreased over the course of the experiment (Fig. 1), indicating that fermentation generally occurred regardless of fiber source. However, the mean final pH ranged from 5.14 for kabocha squash flesh to 6.75 for radish bulb, suggesting that this pooled microbial community could not fully ferment all fibers. In order to determine if fiber monosaccharide composition contributed to the observed variance in the extent of fermentation, we modeled the effect of monosaccharide content on the final pH with generalized linear regression (Table 1). The resulting model found that glucose content was significantly associated with a lower final pH, while xylose content was significantly associated with a higher final pH. Initial pH was not predictive of final pH, suggesting that monosaccharide composition was an important determinant of fermentation. Since glucose was the predominant sugar in most fibers, we assessed if total monosaccharide content was equally predictive of final pH and found that the more nuanced model was slightly superior [Akaike information criterion (AIC) = 53.821 for the model summarized in Table 1 and AIC = 54.969 for the model based on total monosaccharide content].

Since monosaccharide content was found to influence the final pH of fiber fermentations, we hypothesized that pH differences resulted from variation in the SCFAs produced by the gut microbiota during the metabolism of distinct carbohydrate structures. After each 72-hour fermentation, the final concentrations of 19 carboxylic acid metabolites were measured by LC-MS/MS after derivatization (see Materials and Methods). We built a regression tree (Fig. 2) to infer the contributions of individual SCFAs to final pH. Comparison of observed and predicted values (r-squared = 0.471, root-mean-square error = 0.311, and mean absolute error = 0.268) supported our hypothesis that specific SCFAs influenced final pH, with lower pH concentrations predicted by higher concentrations of lactic acid, propionic acid, and indole-3-acetic acid.

Given that specific members of the pooled gut microbiota differ in their ability to produce SCFAs, we next sought to identify how the composition of the initial microbial community changed over the course of fermentation in response to variation in monosaccharide composition. Four samples (0, 24, 48, and 72 hours) were taken from each fermentation for 16S rRNA sequencing. The relative abundance of microbial families (Fig. 3) was generally similar for 0-hour samples, suggesting that the initial conditions

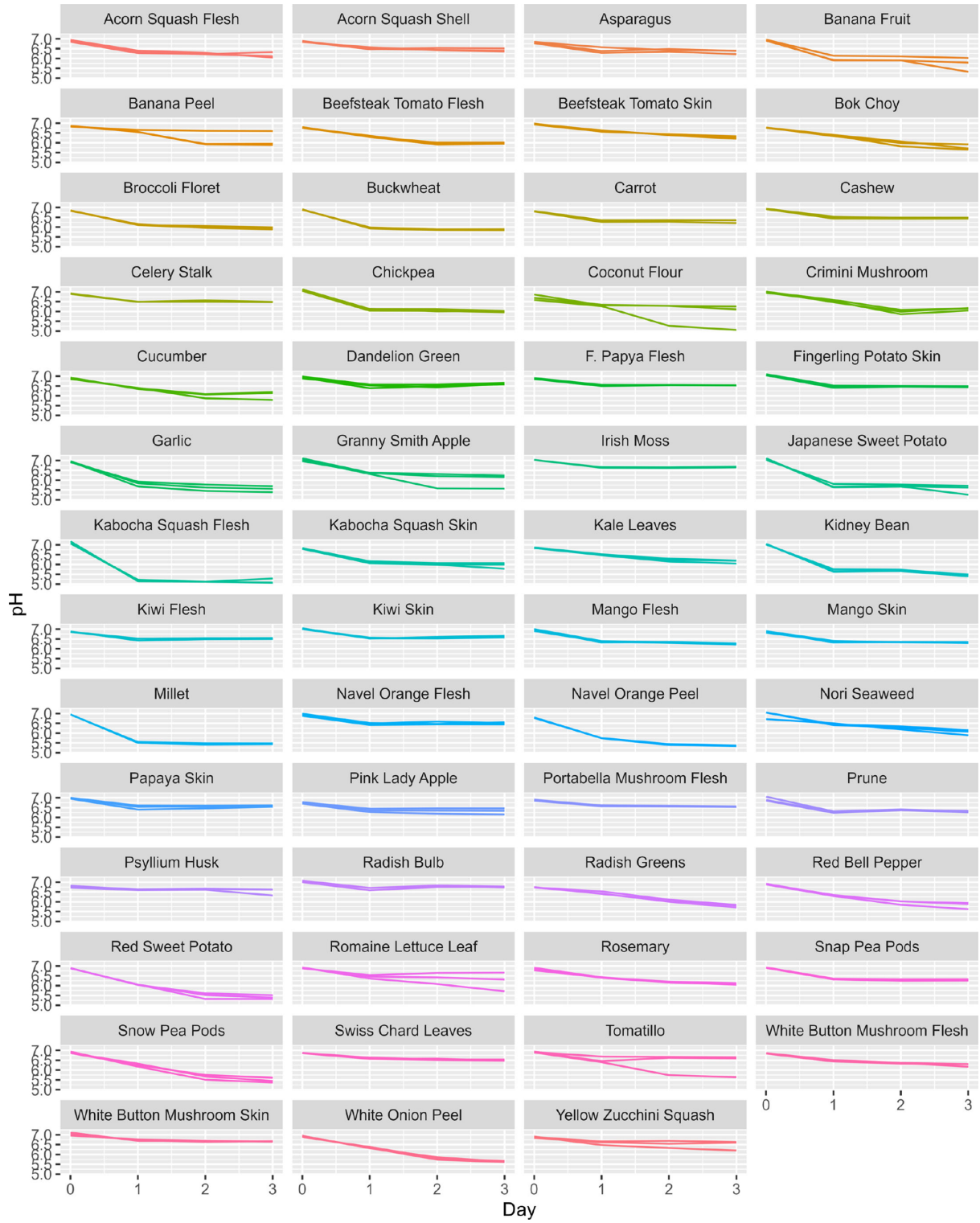

FIG 1 pH change over the course of 3 days (72 hours) food fiber fermentations. pH was measured every day (24 hours). Lines show mean ±2 SD. Food fibers were processed as described Materials and methods.

of each fermentation did not vary considerably. Differences in relative abundance were apparent between fiber sources in 24–72 hour samples. The alpha diversity (richness and evenness) of microbiome samples was quantified with the Shannon index after rarefaction to a depth of 2,509 reads, which retained 1,881,750 features (15.56% of

TABLE 1 Generalized linear model to predict final pH from fiber monosaccharide composition[a]

Variable	Transformation	Beta-coefficient	95% CI	*P*-value
Intercept	NA	6.469	6.196–6.742	<2e-16
Glucose	Box-Cox	−0.0216	−0.0407 to −0.00260	0.0267
Xylose	Box-Cox	0.125	0.0200–0.230	0.0206
Rhamnose	Box-Cox	−0.656	−1.509 to −0.197	0.129

[a]The influence of each variable on final pH was assessed with purposeful selection modeling. Box-Cox transformations were applied to monosaccharide data due to deviations from normality. Rhamnose was included in the model as a confounder of xylose. Monosaccharide data were scaled by minimum and maximum values.

features) in 750 samples (92.59% of samples). A LME model (Table 2) found that baseline alpha diversity was not predictive of longitudinal alpha diversity at 24–72 hours. However, xylose was significantly associated with lower alpha diversity, while rhamnose, GalA, and GlcA were significantly associated with higher alpha diversity, suggesting that the composition of the microbial community changed due to differences in monosaccharide content.

To determine if observed differences in alpha diversity were accompanied by functional differences, we built a regression tree (Fig. 4) to predict the alpha diversity of unknown samples based on the concentration of SCFAs. Comparison of observed and predicted values (*r*-squared = 0.675, root-mean-square error = 0.306, and mean absolute error = 0.231) indicated that final alpha diversity was predicted by lactic acid and propionic acid, with higher lactic acid concentration associated with a lower final alpha diversity and higher propionic acid concentration associated with higher final alpha diversity.

Since differences in alpha diversity may be accompanied by alterations in the structure of the microbiome, we tested for dissimilarity between microbiome samples from different fermentations (beta-diversity). A distance matrix of Bray–Curtis distances between microbiome samples was calculated. PERMANOVA of the Bray–Curtis distance matrix indicated that the content of the monosaccharides glucose, galactose, fructose, rhamnose, GalA, GalNac, mannose, and allose, as well as sequencing run, were all significantly associated with the dissimilarity of microbiome samples after 72 hours of fermentation (Table 3). Results from 24 and 48 hours were similar to those at 72

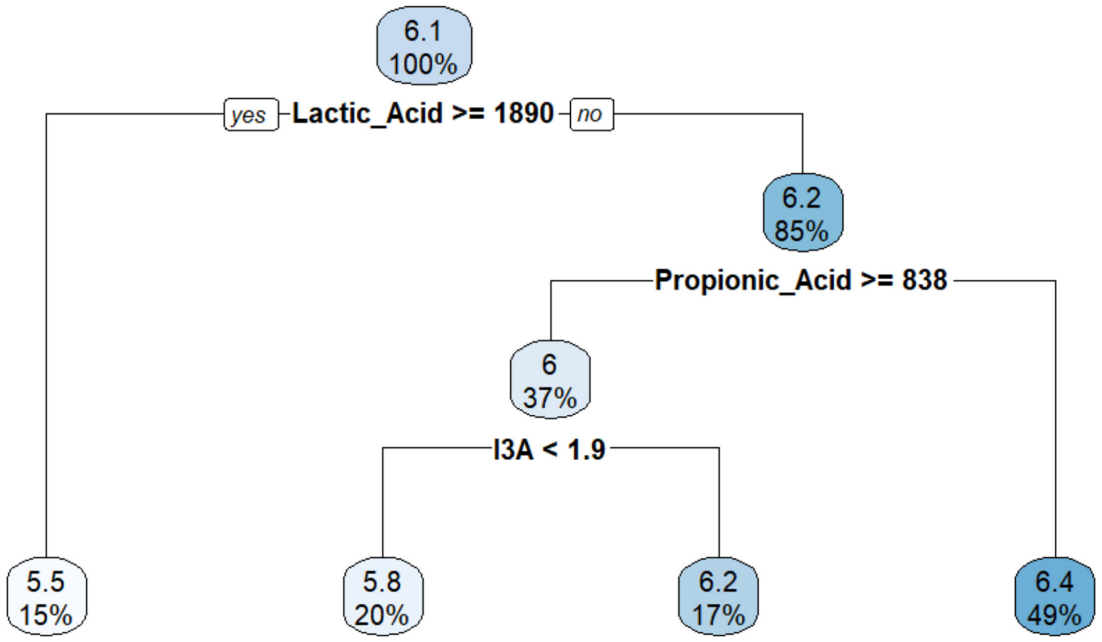

FIG 2 Regression tree predicting pH from SCFA levels of fecal fermentations. I3A, indole-3-acetic acid. Color intensity reflects the predicted pH of that node (darker equals a higher pH value).

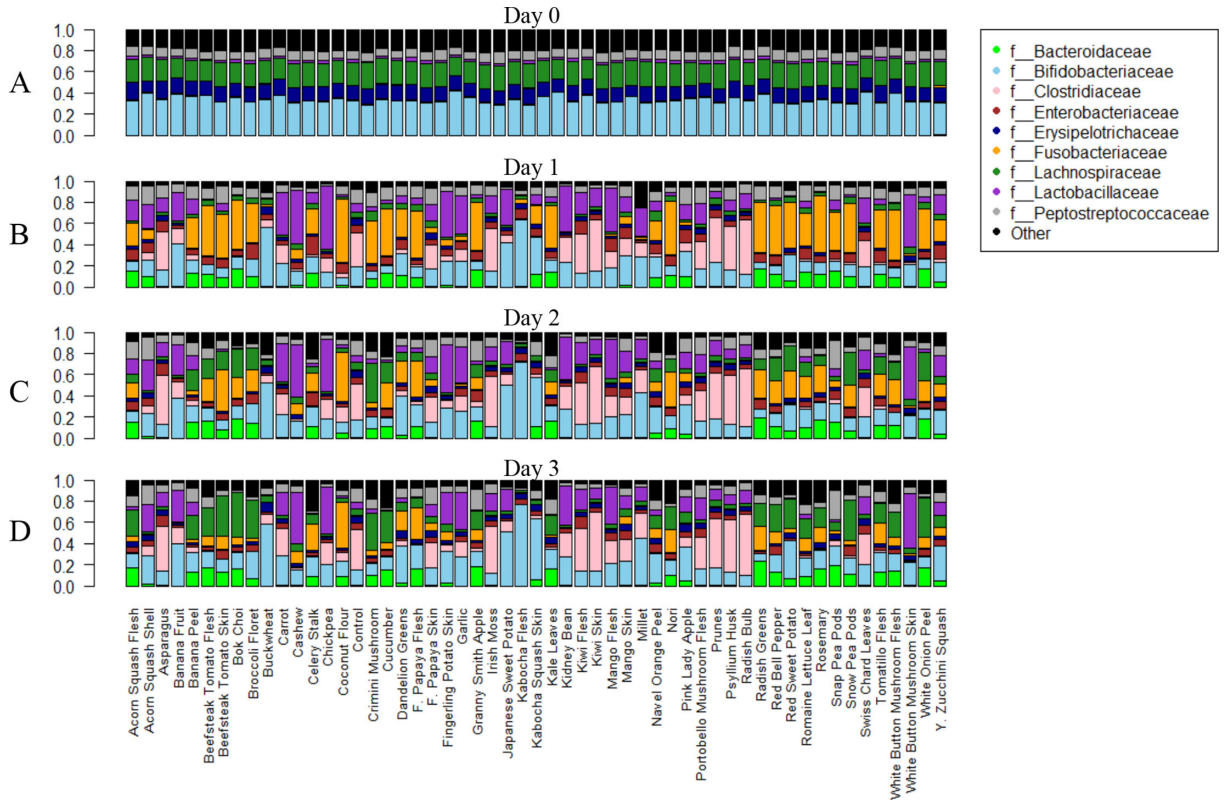

FIG 3 Average relative abundance of microbial taxa by fiber source at each time point of fecal fermentation. Panel A, Day 0; Panel B, Day 1; Panel C, Day 2; Panel D, Day 3. Fiber sugar monomer compositions are shown in Table S1.

hours, with GlcA also a significant variable at 24 hours, while sequencing run was the only significant variable at 0 hours (Table S4). These results suggest that many monosaccharides independently influenced microbial community structure over the course of fermentation. Ordination with NMDS was performed to visualize 72-hour samples according to their Bray–Curtis distances. Ordinations with points colored using a gradient based on fiber monosaccharide content (Fig. 5A) generally agreed with PERMANOVA results, suggesting that samples from the fermentation of fibers with high levels of each monosaccharide were often similar, as measured by Bray-Curtis distance. A gradient plot of final pH (Fig. 5B) suggested that samples with similar final pH levels also tended to be similar, as measured by Bray-Curtis distance.

Given differences in microbiome composition and structure were evident between fermentations, we next sought to identify which specific microbial genera responded to differences in fiber monosaccharide content and contributed to the observed final pH differences. Quantitative fiber monosaccharide data were classified into tertiles to test for differentially abundant taxa with ANCOM. ANCOM results at the genus level

TABLE 2 Linear mixed effects model to predict longitudinal alpha diversity[a]

Variable	Estimate	95% CI	*P*-value
Intercept	2.190	2.090–2.290	<2e-16
Day	0.136	0.105–0.166	<2e-16
Xylose	−0.00708	−0.0127 to −0.00143	0.0145
Rhamnose	0.149	0.0941–0.204	2.99e-07
GalA	0.0394	0.0238–0.0550	1.71e-06
GlcA	0.609	0.100–1.118	0.0195

[a]The model included baseline alpha diversity and each monosaccharide as a fixed effect and bioreactor ID as a random effect. Modeling was performed with lme4. Monosaccharide data were normalized by scaling from 0 to 1.

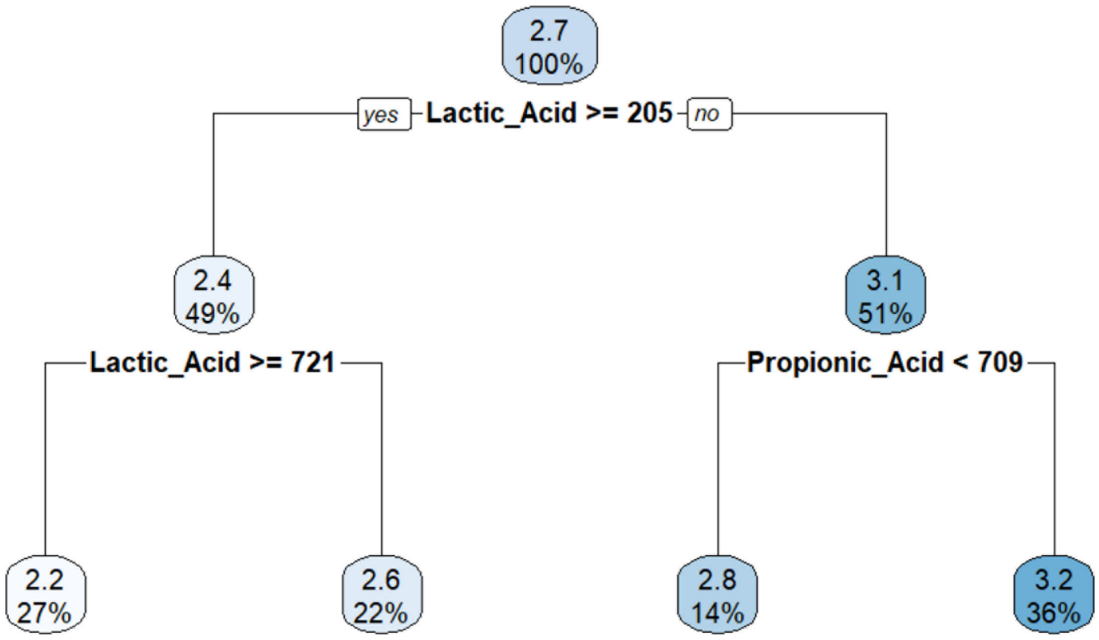

FIG 4 Regression tree of association of SCFA with alpha diversity. Color intensity reflects higher predicted alpha diversity.

(Table 4) suggest that differences in the content of 11 monosaccharides were associated with significant differences in the relative abundance of 11 microbial genera, including *Lactobacillus*, *Flavonifractor*, and *Lachnospira*. Notably, the genus *Dubosiella* was enriched in fermentations of fibers with higher levels of three monosaccharides: allose, GalNac, and GlcA. Higher GalA content was significantly associated with the relative abundance of three genera: *Libanicoccus*, *Alistipes*, and *Phocea*. In order to determine if any of these genera contributed to observed differences in microbiome function, 72-hour fermentations containing different tertiles of SCFAs were also tested for the differential abundance of microbial genera with ANCOM (Table 5). The relative abundance of *Lactobacillus*, *Flavonifractor*, *Lachnospira*, *Libanicoccus*, *Alistipes*, and *Phocea* was significantly associated with the concentration of both lactic acid and propionic acid. Additionally, the relative abundance of *Dubosiella* was significantly associated with I3B concentration. Our results suggest that variation in fiber monosaccharide content influences both the community composition and metabolic output of a model gut microbiota.

Briefly, we found significant differences in alpha diversity, beta diversity, and microbial community diversity and structure after 72 hours of fermentation based on fiber monosaccharide composition. Final pH was significantly associated with fiber glucose,

TABLE 3 Day 3 PERMANOVA of microbiome data from 72-hour fermentation samples[a]

Variable	*P*-value
Sequencing run	0.003
Glucose	0.015
Galactose	0.033
Fructose	0.013
Rhamnose	0.004
GalA	0.001
GalNac	0.009
Mannose	0.001
Allose	0.016

[a]PERMANOVA was performed with 999 permutations on distance matrics of Bray-Curtis distances with the adonis2 function (vegan package). Rarefied 16S rRNA sequence data (rarefraction depth = 2,509) were used due to >10-fold read differences between samples.

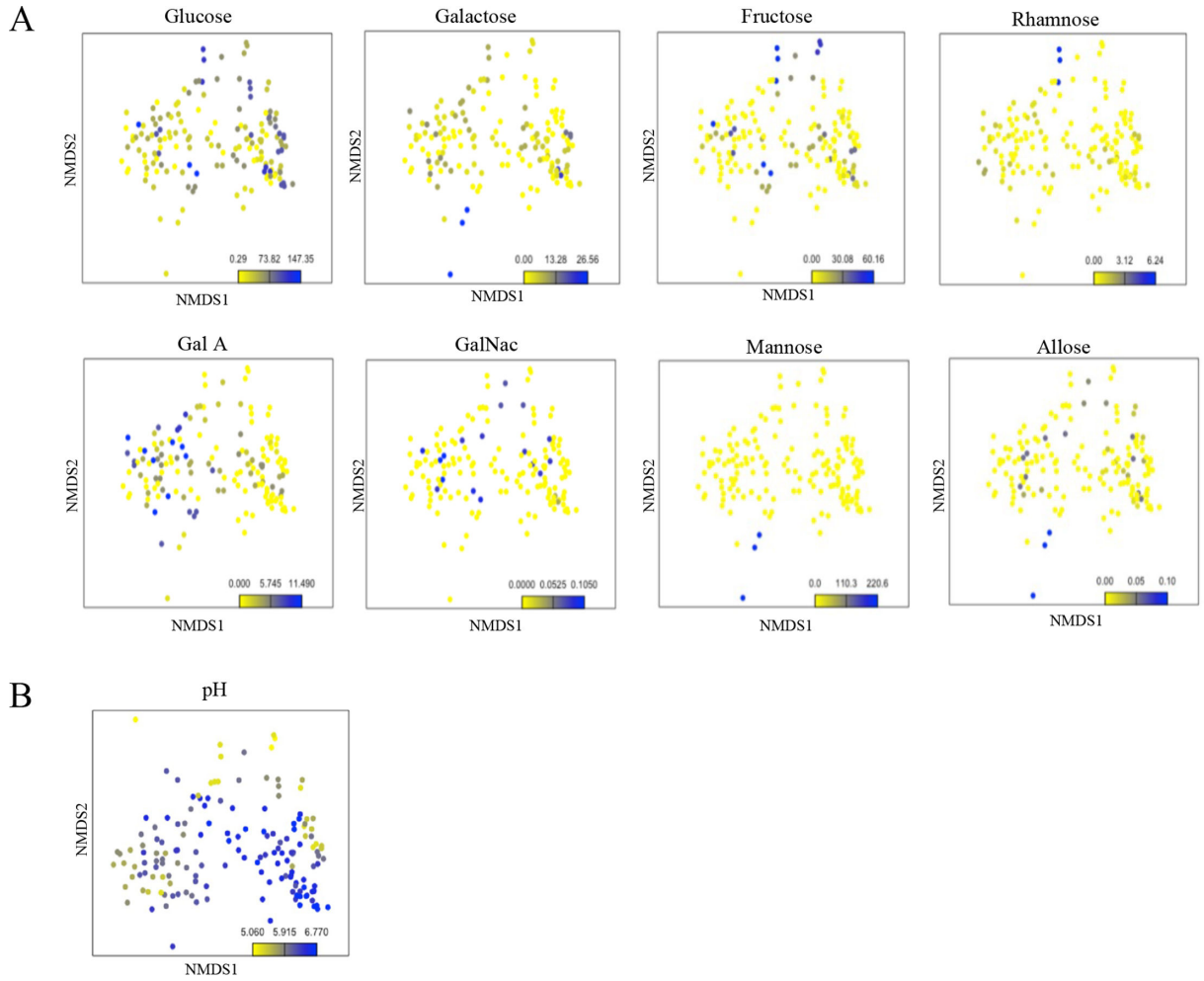

FIG 5 Gradient plots of microbiome samples after 72 hours (day 3) of fermentation. Ordination was performed with NMDS of a matrix of Bray-Curtis distances (two dimensions and stress 0.1525762). (A) Individual monosaccharide component of food fibers used in fermentations. (B) Final pH.

rhamnose, and xylose content and was predictable from lactic acid and propionic acid concentrations. The relative abundance of several genera, including *Lactobacillus* and *Dubosiella*, were significantly associated with both individual fiber monosaccharides and final short-chain fatty acid concentrations.

DISCUSSION

The composition of the colonic microbiota of mammals is shaped in large part by the ingestion of dietary fibers (57), with glycan complexity determining the extent to which individual microbes can process these polysaccharides or their oligosaccharide components (58). Complex dietary glycans are known to nourish extended "food chains" in the mammalian gut, with primary degraders such as *Bacteroides* spp. encoding polysaccharide utilization loci to recognize and break down specific structures, releasing byproducts that support downstream niches such as secondary degraders and acetogens (59). Dietary fibers were recently shown to vary in the specificity of the changes they induce in microbial community structure, with simple, common fibers like fructooligosaccharides inducing less dramatic and less selective changes than rarer, insoluble fibers such as *β*-glucan (60). However, though carbohydrates may be studied with a variety of analytical methods, such as ion mobility spectrometry and gas-phase spectroscopy (61), the complexity of food glycans has precluded detailed understanding of their structure. An ultra-high performance liquid chromatography triple quadrupole

TABLE 4 ANCOM results for fiber monosaccharide data, including monosaccharide (Sugar), associated taxa (Genus), centered log ratio (CLR), and W statistic[a]

Sugar	Genus	CLR	W statistic
Allose	Dubosiella	23.43	97
Fructose	[Eubacterium] brachy group	11.04	54
GalA	Libanicoccus	9.65	81
GalA	Alistipes	8.35	73
GalA	Phocea	9.72	71
Galactose	UVBA1819	10.83	73
GalNac	Dubosiella	57.41	107
GlcA	Dubosiella	23.83	93
Glucose	Holdemanella	8.81	41
Mannose	Clostridium *sensu stricto* 1	21.6	119
Rhamnose	Lactobacillus	9.54	108
Ribose	Flavonifractor	9.3	67
Xylose	Lachnospira	12.06	118

[a]16S rRNA sequencing data taken after 72 hours of fermentation were tested for differential abundance based on fiber monosaccharide content. Monosaccharide data were classified into tertiles, and sequencing data were analyzed at the genus level.

mass spectrometry approach developed by the Lebrilla and coworkers (30) expands on existing methods in both breadth and depth. Examples of the detailed monosaccharide composition data obtained with this method have been published in the Davis Food Glycopedia (31) for hundreds of common dietary carbohydrate sources, offering relevant structural information for ongoing studies that examine the impact of diet on the human gut microbiota. Similarities or differences in chemical structure may not be intuitively obvious; for example, hierarchical clustering suggested that the monosaccharide compositions of red sweet potato and Japanese sweet potato were relatively distinct, whereas seemingly unrelated food fibers such as buckwheat and radish bulb were similar. These examples suggest that qualitative dietary diversity may not reflect underlying structural diversity, with possible ramifications for studies that seek that examine the gut microbiota's response to broad dietary patterns, such as the Mediterranean diet (62) or whole-grain consumption (63).

The present study takes advantage of the data in the Davis Food Glycopedia and directly links variation in monosaccharide composition to the outcome of fermentation by the gut microbiome. Modeling revealed that glucose content was the variable most predictive of the final pH of fermentation, a result that likely reflects the wide distribution of glucosidases in the mammalian gut microbiome (64, 65). While a model based on total monosaccharide content performed almost as well as one based on glucose and xylose content, several individual monosaccharides were significantly associated with microbial alpha and beta diversity and community composition, suggesting that total monosaccharide content inadequately reflects gut microbial fermentation. The capacity for metabolism of less abundant monosaccharides may be common across the microbiome but variable within taxa; for example, only certain *Bifidobacterium* and *Bacteroides* strains encode sialidases (66), but sialidases and their associated catabolic pathways were found in 80/397 genomes analyzed from the Human Microbiome Project (67). Modeling found that xylose content was significantly associated with a higher final pH and a lower alpha diversity. This result may reflect a relative paucity of enzymes for metabolizing xylose-containing carbohydrates in the microbiome inoculum. Alternatively, it is possible that xylose metabolism is relatively common, but xylose-rich foods support the growth of a narrower range of microbes. This may be due to competition between microbes, leading to reduced net fermentation and alpha diversity. This is plausible because common microbes such as *Prevotella* and *Bacteroides* are known to metabolize xylans and arabinoxylans (9, 24, 25), but the fine structure of xylose-containing oligosaccharides may govern antagonistic regulation of bacterial carbohydrate-active enzymes (68) and the ability of secondary degraders to consume xylooligosaccharide breakdown

TABLE 5 ANCOM results for acidic microbial metabolites (AMMs)[a]

AMM	Genus	CLR	W statistic
Propionic acid	Clostridium *sensu stricto* 1	65.31	118
Propionic acid	Lactobacillus	55.24	118
Propionic acid	Romboutsia	45.88	117
Propionic acid	Alistipes	46.34	113
Propionic acid	[Ruminococcus] torques group	34.57	113
Propionic acid	Colidextribacter	51.11	112
Propionic acid	Unknown genus of family Lachnospiraceae	41.14	111
Propionic acid	Bacteroides	39.72	110
Propionic acid	Peptococcus	29.98	108
Propionic acid	Solobacterium	33.34	108
Propionic acid	[Ruminococcus] gauvreauii group	33.49	107
Propionic acid	Coprococcus	31.29	105
Propionic acid	RF39	28.64	104
Propionic acid	Dialister	28.14	101
Propionic acid	Lachnospira	20.19	100
Propionic acid	Butyricimonas	23.85	99
Propionic acid	Oscillibacter	27.48	99
Propionic acid	Libanicoccus	23.47	99
Propionic acid	Negativibacillus	23.88	98
Propionic acid	Parabacteroides	19.60	97
Propionic acid	Odoribacter	17.77	97
Propionic acid	Enterococcus	16.34	97
Propionic acid	Muribaculaceae	12.46	95
Propionic acid	Fusicatenibacter	12.88	95
Propionic acid	[Clostridium] methylpentosum group	11.73	94
Propionic acid	Sutterella	28.04	94
Propionic acid	Uncultured	14.78	94
Propionic acid	Butyricicoccus	11.24	94
Propionic acid	[Ruminococcus] gnavus group	12.86	93
Propionic acid	Lachnoclostridium	11.07	93
Propionic acid	Barnesiella	6.60	92
Propionic acid	Phocea	11.19	92
Propionic acid	Uncultured genus of family Desulfovibrionaceae	8.81	89
Propionic acid	Flavonifractor	8.36	89
Propionic acid	Fusobacterium	9.32	88
Lactic acid	Clostridium *sensu stricto* 1	40.70	119
Lactic acid	Lactobacillus	63.10	119
Lactic acid	Romboutsia	47.60	118
Lactic acid	Unknown genus of family Lachnospiraceae	72.04	117
Lactic acid	[Ruminococcus] torques group	63.04	116
Lactic acid	Alistipes	74.12	115
Lactic acid	Bacteroides	76.81	113
Lactic acid	Lachnospira	26.73	109
Lactic acid	Enterococcus	27.72	109
Lactic acid	Colidextribacter	40.27	109
Lactic acid	Subdoligranulum	29.17	108
Lactic acid	[Ruminococcus] gauvreauii group	37.16	107
Lactic acid	Coprococcus	30.29	106
Lactic acid	Solobacterium	34.58	106
Lactic acid	Dialister	27.25	102
Lactic acid	Butyricimonas	47.84	102
Lactic acid	Oscillibacter	38.21	101

(*Continued on next page*)

TABLE 5 ANCOM results for acidic microbial metabolites (AMMs)[a] (*Continued*)

AMM	Genus	CLR	W statistic
Lactic acid	Fusobacterium	22.46	101
Lactic acid	Peptococcus	19.79	100
Lactic acid	Parabacteroides	17.94	100
Lactic acid	Libanicoccus	27.79	99
Lactic acid	Lachnospiraceae	11.09	99
Lactic acid	Uncultured genus of family Desulfovibrionaceae	18.03	98
Lactic acid	UBA1819	9.74	98
Lactic acid	Phocea	17.09	97
Lactic acid	Odoribacter	16.69	97
Lactic acid	Flavonifractor	16.38	96
Lactic acid	Negativibacillus	19.64	95
Lactic acid	[Ruminococcus] gnavus group	14.21	95
Lactic acid	Uncultured	10.28	95
Lactic acid	Sutterella	13.87	94
Lactic acid	Butyricicoccus	9.59	92
Indole-3-butyric acid	Dubosiella	8.30	53
I3A	Mogibacterium	11.01	44
I3A	Collinsella	10.23	39

[a]16S rRNA sequencing data taken after 72 hours of fermentation were tested for differential abundance based on tertiles of each AMM in the corresponding fermentor. Sequencing data were analyzed at the genus level. Only taxa where the null hypothesis is rejected after false discovery rate adjustment (FDR) are shown.

products (58). Further supporting this possibility, a recent study showed that related *Prevotella* spp. competed for arabinoxylan, with *P. intestinalis* outcompeting *P. rodentium* and *P. muris* (69). A randomized controlled trial showed that arabinoxylan reduced LDL and total cholesterol (70). Additionally, *Bacteroides* that metabolize arabinoxylans have been shown to release the antioxidant ferulic acid (25, 71), suggesting that gut microbial xylose metabolism may have implications for health. In contrast to xylose, the less abundant sugars rhamnose, GalA, and GlcA were significantly associated with a higher alpha diversity. Structures containing these rarer monosaccharides may support a higher alpha diversity by providing a higher selectivity (17), creating many unfilled ecological niches. Future research should identify carbohydrate-active enzymes that process structures containing rhamnose, GalA, and GlcA to determine which microbes are capable of metabolizing them.

Fermentation pH and microbial diversity were also found to reflect variation in SCFAs, which are known to affect microbial ecology. While changes in dietary fiber consumption are known to rapidly alter SCFA production by the mammalian gut microbiota, such as that of beagles (72), the metabolic fluxes that convert individual dietary monosaccharides into SCFAs are poorly understood. A recent study suggested that SCFAs such as succinic acid, propionic acid, and butyric acid differentially inhibited gut Bacteroidales, but sensitivity to butyric acid depended on the provision of specific carbohydrates (73). This work found that final pH was strongly associated with the levels of acetic acid, possibly because acetic acid is the most widely produced SCFA in the gut [the molar ratio of acetic acid:propionic acid:butyric acid is 60:20:20 (12)]. This finding is consistent with other work, for example, a reduction in mouse cecal pH mediated by the production of acetic acid by *Bifidobacterium* was shown to protect against infection by *Escherichia coli* O157:H7 (74). In addition to the association with acetic acid, propionic acid was associated with a lower final pH and with differences in the relative abundance of 35 genera. Using regression trees, higher propionic acid was also predictive of higher alpha diversity, while lactic acid was predictive of lower alpha diversity. While propionic acid is less studied than butyric acid and acetic acid, it was found to increase in human subjects fed corn bran arabinoxylan (75) and has been shown to mediate colonization resistance to *Salmonella* infection in a mouse model (76), suggesting that future studies should examine its production by genera identified here, such as *Lactobacillus* and *Romboutsia*.

Propionic acid is produced by multiple routes, including from succinate and via the acrylate pathway (77), possibly explaining why numerous genera were significantly associated with propionic acid levels. While many studies have examined the production of SCFAs by the gut microbiota, the present study also examined a broader range of acidic microbial metabolites. I3A was also found to be significantly associated with a lower final pH, while I3P was significantly associated with the relative abundance of 28 microbial genera, suggesting that it may be produced by a variety of gut bacteria. These indole derivatives are bioactive: I3P signals through the pregnane X receptor to maintain intestinal barrier integrity (78), while I3A signals via the aryl hydrocarbon receptor and may reduce liver inflammation (79). However, the relationship between host diet, microbial metabolism, and the production of these metabolites remains unclear. In the production of acidic microbial metabolites, there is a role for the production of both primary degraders that directly convert food polysaccharides to produce metabolites and "cross-feeders" who produce metabolites by taking up and breaking down byproducts released by primary degraders (80). As an example of cross-feeding, the genome of the butyrate producer *Faecalibacterium prausnitzii* encodes two loci for catabolizing mannooligosaccharides liberated by primary degradation of *β*-mannans (81). While our study identified several genera whose relative abundance was significantly associated with monosaccharide content and acidic microbial metabolite levels, such associations may be indirect and depend on interspecific ecological interactions, such as cross-feeding and competition. Future studies should trace the microbial origins of these metabolites in order to establish the foci at which variation in dietary monosaccharide content affects microbial food webs.

The factors that influence both food carbohydrate structure and the ecology of the gut microbiota are multifactorial, so understanding their relationship is challenging. This study suggests that monosaccharide composition provides a generalizable metric for comparing dietary carbohydrates and identifying the functional roles of individual members of the microbiota. The principle of competitive exclusion suggests that each microbe must realize a distinct niche in the gut ecosystem, but this situation may be achieved by multiple possible mechanisms, such as alternative gene regulation and enzymatic specificity (8). Microbes may also exhibit metabolic flexibility; in a study *Bacteroides cellulolyticus* competed with *Bacteroides vulgatus* for arabinan, but competition for arabinoxylan between *B. celluloyticus* and *Bacteroides ovatus* did not occur because *B. ovatus* priorritized alternate glycans (16). Despite the complexities of such interactions, monosaccharide composition offers a resource for the large-scale analysis of dietary carbohydrate structure in order to help untangle the mechanisms by which gut bacteria metabolize microbiota-accessible carbohydrates. Our study used a pooled, feline fecal sample with a modified feline artificial digestion process to maximize the microbial accessible carbohydrate content in our experiment, leading to a successful demonstration of the reproducibility of a bioreactor-based system for analyzing the response of a mammalian microbiota to a large set of dietary fibers. This system allows the impact of carbohydrate structure to be examined independently of host factors. We identified little-studied significant associations between monosaccharide content and the relative abundance of specific genera, such as the significant association between higher GalA content and the relative abundance of *Libanicoccus*, *Alistipes*, and *Phocea*. While *Phocea* and *Libanicoccus* have been isolated from human stool (82, 83), they are poorly studied and may merit further investigation in relation to diet and metabolism. In contrast, the genus *Alistipes* is well-known within the human gut for its bile tolerance (84) and ability to perform protein putrefaction (85), but its response to dietary fibers containing GalA has not been studied. Analysis of monosaccharide composition provides a simple way to identify many such potential links between dietary carbohydrate structure and specific gut bacteria. Examples to guide future mechanistic research include past studies that have demonstrated how individual gut bacteria consume HMOs (86), mucins (87, 88), algal porphyrans (7), red seaweed agarose (89), β-mannans (81), and acetylated galactoglucomannans and arabinoglucuronoxylans (15, 90).

Our study thus provides an initial framework for analyzing dietary monosaccharide intake as one of several factors that contribute to the mechanisms of gut microbial metabolism. Future studies may exploit emerging methods, such as chemical and isotopic labeling, in order to trace the fate of individual dietary monosaccharides in single microbial cells (91). While our work identified monosaccharide content as a determinant of fermentation, future studies should examine other facets of carbohydrate structure that are known to affect microbial metabolism, such as linkages (92) and chemical modifications (23, 93). In particular, different glycosyl hydrolases cleave select linkages between monosaccharides, which are critical to defining the microbes capable of consuming a fiber. For example, different microbes are known to have different genetic machinery to digest starches (6) and can enable keystone degraders, who complete external initial cleavage of the starch, to cross-feed secondary degraders (94). As a result, an enhanced understanding of both fiber monomer and linkage content will be critical to understanding microbiome-fiber interaction networks. A recent study supporting this concept compared the human gut microbiome's response to arabinan-rich pea fiber and homogalacturonan-rich orange fiber *in vivo* and found that changes in carbohydrate-active enzyme content were negatively correlated with the glycosidic linkages they targeted (95). This argues that monosaccharides should be considered within their broader structural context. More nuanced structural analysis may also use liquid chromatography-mass spectrometry to identify oligosaccharides produced by the cleavage of polysaccharides (96) in order to predict which secondary degraders may be able to exploit the breakdown of dietary glycans. Fiber monosaccharide data may provide input for deep-learning algorithms to predict microbial responses to diet (97). Eventually, knowledge of the intimate relationships between carbohydrate structure and the metabolism of individual microbes may permit the development of more personalized "microbiota-directed foods" (98) that target functional outcomes, such as the production of bioactive microbial metabolites or changes in the host's plasma proteome (99). A recent human crossover trial found that butyrate production by the gut microbiota in response to the simple glycans inulin, galactooligosaccharides, and dextrin was limited by an individual's habitual fiber intake (100), suggesting that future interventions may be more successful if they exploit a deeper understanding of dietary fiber structure to identify gaps in the structural diversity of personalized human diets.

ACKNOWLEDGMENTS

Funding for this work was provided by Mars Inc., NIH grants R01DK124193 (C.B.L.) and F32HD093185 (D.H.T.), and the Bill and Melinda Gates Foundation (D.A.M.). N.J. was supported in part on a Danone North America Gut Microbiome, Yogurt and Probiotics Fellowship.

AUTHOR AFFILIATIONS

[1]Department of Food Science and Technology, University of California, Davis, California, USA
[2]Foods for Health Institute, University of California, Davis, California, USA
[3]Department of Chemistry, University of California, Davis, California, USA
[4]Department of Food Science and Human Nutrition, University of Florida, Gainsville, Florida, USA

PRESENT ADDRESS

Maria Maldonado-Gomez, one.bio, Sacramento, California, USA
Juan Castillo, Gilead Sciences, Inc., Foster City, California, USA

AUTHOR ORCIDs

David A. Mills http://orcid.org/0000-0003-1913-9865

Diana H. Taft http://orcid.org/0000-0002-9306-9968

FUNDING

Funder	Grant(s)	Author(s)
Mars (Mars Incorporated)		David A. Mills
HHS | NIH | National Institute of Diabetes and Digestive and Kidney Diseases (NIDDK)	R01DK124193	Carlito B. Lebrilla
Bill and Melinda Gates Foundation (GF)		David A. Mills
Gut Microbiome Yogurt and Probiotics Fellowship		Nick Jensen
HHS | National Institutes of Health (NIH)	F32HD093185	Diana H. Taft

AUTHOR CONTRIBUTIONS

Nick Jensen, Data curation, Investigation, Writing – original draft | Maria Maldonado-Gomez, Data curation, Formal analysis, Investigation, Methodology, Supervision, Validation, Writing – review and editing | Nithya Krishnakumar, Data curation, Investigation, Methodology, Validation, Writing – review and editing | Cheng-Yu Weng, Data curation, Investigation, Methodology, Writing – review and editing | Juan Castillo, Data curation, Formal analysis, Methodology | Dale Razi, Investigation, Methodology | Karen Kalanetra, Investigation, Methodology, Supervision | J. Bruce German, Conceptualization, Supervision, Writing – review and editing | Carlito B. Lebrilla, Conceptualization, Funding acquisition, Supervision, Writing – review and editing | David A. Mills, Conceptualization, Data curation, Funding acquisition, Project administration, Writing – review and editing | Diana H. Taft, Conceptualization, Data curation, Formal analysis, Investigation, Methodology, Writing – original draft, Writing – review and editing

DATA AVAILABILITY

Sequencing data from this project are available on NCBI SRA, accession PRJNA1127241.

ADDITIONAL FILES

The following material is available online.

Supplemental Material

Figure S1 (AEM00964-24-s0001.tiff). Hierarchical clustering analysis of 55 food fibers based on absolute monosaccharide composition.
Supplemental tables (AEM00964-24-s0002.pdf). Tables S1 to S4.

REFERENCES

1. Schmidhuber J, Sur P, Fay K, Huntley B, Salama J, Lee A, Cornaby L, Horino M, Murray C, Afshin A. 2018. The global nutrient database: availability of macronutrients and micronutrients in 195 countries from 1980 to 2013. Lancet Planet Health 2:e353–e368. https://doi.org/10.1016/S2542-5196(18)30170-0
2. Slavin J, Carlson J. 2014. Carbohydrates. Adv Nutr 5:760–761. https://doi.org/10.3945/an.114.006163
3. Sonnenburg ED, Sonnenburg JL. 2014. Starving our microbial self: the deleterious consequences of a diet deficient in microbiota-accessible carbohydrates. Cell Metab 20:779–786. https://doi.org/10.1016/j.cmet.2014.07.003
4. Sonnenburg ED, Smits SA, Tikhonov M, Higginbottom SK, Wingreen NS, Sonnenburg JL. 2016. Diet-induced extinctions in the gut microbiota compound over generations. Nature 529:212–215. https://doi.org/10.1038/nature16504
5. Flint HJ, Scott KP, Duncan SH, Louis P, Forano E. 2012. Microbial degradation of complex carbohydrates in the gut. Gut Microbes 3:289–306. https://doi.org/10.4161/gmic.19897
6. Ndeh D, Gilbert HJ. 2018. Biochemistry of complex glycan depolymerisation by the human gut microbiota. FEMS Microbiol Rev 42:146–164. https://doi.org/10.1093/femsre/fuy002
7. Robb CS, Hobbs JK, Pluvinage B, Reintjes G, Klassen L, Monteith S, Giljan G, Amundsen C, Vickers C, Hettle AG, Hills R, Xing X, Montina T, Zandberg WF, Abbott DW, Boraston AB, Nitin. 2022. Metabolism of a hybrid algal galactan by members of the human gut microbiome. Nat Chem Biol 18:501–510. https://doi.org/10.1038/s41589-022-00983-y
8. Lindemann SR. 2020. A piece of the pie: engineering microbiomes by exploiting division of labor in complex polysaccharide consumption. Curr Opin Chem Eng 30:96–102. https://doi.org/10.1016/j.coche.2020.08.004
9. Aakko J, Pietilä S, Toivonen R, Rokka A, Mokkala K, Laitinen K, Elo L, Hänninen A. 2020. A carbohydrate-active enzyme (CAZy) profile links successful metabolic specialization of *Prevotella* to its abundance in gut microbiota. Sci Rep 10:12411. https://doi.org/10.1038/s41598-020-69241-2

10. Cartmell A, Muñoz-Muñoz J, Briggs JA, Ndeh DA, Lowe EC, Baslé A, Terrapon N, Stott K, Heunis T, Gray J, Yu L, Dupree P, Fernandes PZ, Shah S, Williams SJ, Labourel A, Trost M, Henrissat B, Gilbert HJ. 2018. A surface endogalactanase in *Bacteroides thetaiotaomicron* confers keystone status for arabinogalactan degradation. Nat Microbiol 3:1314–1326. https://doi.org/10.1038/s41564-018-0258-8
11. Chung WSF, Walker AW, Louis P, Parkhill J, Vermeiren J, Bosscher D, Duncan SH, Flint HJ. 2016. Modulation of the human gut microbiota by dietary fibres occurs at the species level. BMC Biol 14:3. https://doi.org/10.1186/s12915-015-0224-3
12. den Besten G, van Eunen K, Groen AK, Venema K, Reijngoud D-J, Bakker BM. 2013. The role of short-chain fatty acids in the interplay between diet, gut microbiota, and host energy metabolism. J Lipid Res 54:2325–2340. https://doi.org/10.1194/jlr.R036012
13. Lee J-H, O'Sullivan DJ. 2010. Genomic insights into bifidobacteria. Microbiol Mol Biol Rev 74:378–416. https://doi.org/10.1128/MMBR.00004-10
14. Michalak L, GabyJC, LagosL, La Rosa SL, TerraponN, LombardV, HenrissatB, ArntzenM, HagenLH, DrogeJ, OverlandM, PopePB, WesterengB. 2019. Engineered fibre enables targeted activation of butyrate-producing microbiota in the distal gut. bioRxiv. https://doi.org/10.1101/799023
15. Michalak L, Gaby JC, Lagos L, La Rosa SL, Hvidsten TR, Tétard-Jones C, Willats WGT, Terrapon N, Lombard V, Henrissat B, Dröge J, Arntzen MØ, Hagen LH, Øverland M, Pope PB, Westereng B. 2020. Microbiota-directed fibre activates both targeted and secondary metabolic shifts in the distal gut. Nat Commun 11:5773. https://doi.org/10.1038/s41467-020-19585-0
16. Patnode ML, Beller ZW, Han ND, Cheng J, Peters SL, Terrapon N, Henrissat B, Le Gall S, Saulnier L, Hayashi DK, Meynier A, Vinoy S, Giannone RJ, Hettich RL, Gordon JI. 2019. Interspecies competition impacts targeted manipulation of human gut bacteria by fiber-derived glycans. Cell 179:59–73. https://doi.org/10.1016/j.cell.2019.08.011
17. Cantu-Jungles TM, Hamaker BR. 2020. New view on dietary fiber selection for predictable shifts in gut microbiota. mBio 11:e02179-19. https://doi.org/10.1128/mBio.02179-19
18. Tuncil YE, Xiao Y, Porter NT, Reuhs BL, Martens EC, Hamaker BR. 2017. Reciprocal prioritization to dietary glycans by gut bacteria in a competitive environment promotes stable coexistence. mBio 8:e01068-17. https://doi.org/10.1128/mBio.01068-17
19. Deng P, Swanson KS. 2015. Gut microbiota of humans, dogs and cats: current knowledge and future opportunities and challenges. Br J Nutr 113:S6–S17. https://doi.org/10.1017/S0007114514002943
20. Verbrugghe A, Hesta M. 2017. Cats and carbohydrates: the carnivore fantasy? Vet Sci 4:55. https://doi.org/10.3390/vetsci4040055
21. Cerqueira FM, Photenhauer AL, Pollet RM, Brown HA, Koropatkin NM. 2020. Starch digestion by gut bacteria: crowdsourcing for carbs. Trends Microbiol 28:95–108. https://doi.org/10.1016/j.tim.2019.09.004
22. Hamaker BR, Tuncil YE. 2014. A perspective on the complexity of dietary fiber structures and their potential effect on the gut microbiota. J Mol Biol 426:3838–3850. https://doi.org/10.1016/j.jmb.2014.07.028
23. Munoz-Munoz J, Ndeh D, Fernandez-Julia P, Walton G, Henrissat B, Gilbert HJ. 2021. Sulfation of arabinogalactan proteins confers privileged nutrient status to *Bacteroides plebeius*. mBio 12:e0136821. https://doi.org/10.1128/mBio.01368-21
24. Tuncil YE, Thakkar RD, Arioglu-Tuncil S, Hamaker BR, Lindemann SR. 2020. Subtle variations in dietary-fiber fine structure differentially influence the composition and metabolic function of gut microbiota. mSphere 5:e00180-20. https://doi.org/10.1128/mSphere.00180-20
25. Pereira GV, Abdel-Hamid AM, Dutta S, D'Alessandro-Gabazza CN, Wefers D, Farris JA, Bajaj S, Wawrzak Z, Atomi H, Mackie RI, Gabazza EC, Shukla D, Koropatkin NM, Cann I. 2021. Degradation of complex arabinoxylans by human colonic *Bacteroidetes*. Nat Commun 12:459. https://doi.org/10.1038/s41467-020-20737-5
26. Holck J, Hjernø K, Lorentzen A, Vigsnæs LK, Hemmingsen L, Licht TR, Mikkelsen JD, Meyer AS. 2011. Tailored enzymatic production of oligosaccharides from sugar beet pectin and evidence of differential effects of a single DP chain length difference on human faecal microbiota composition after *in vitro* fermentation. Process Biochem 46:1039–1049. https://doi.org/10.1016/j.procbio.2011.01.013
27. Romero Marcia AD, Yao T, Chen M-H, Oles RE, Lindemann SR. 2021. Fine carbohydrate structure of dietary resistant glucans governs the structure and function of human gut microbiota. Nutrients 13:2924. https://doi.org/10.3390/nu13092924
28. Cummings JH, Stephen AM. 2007. Carbohydrate terminology and classification. Eur J Clin Nutr 61:S5–S18. https://doi.org/10.1038/sj.ejcn.1602936
29. Cummings RD, Pierce JM. 2014. The challenge and promise of glycomics. Chem Biol 21:1–15. https://doi.org/10.1016/j.chembiol.2013.12.010
30. Amicucci MJ, Galermo AG, Nandita E, Vo T-TT, Liu Y, Lee M, Xu G, Lebrilla CB. 2019. A rapid-throughput adaptable method for determining the monosaccharide composition of polysaccharides. Int J Mass Spectrom 438:22–28. https://doi.org/10.1016/j.ijms.2018.12.009
31. Castillo JJ, Couture G, Bacalzo NP, Chen Y, Chin EL, Blecksmith SE, Bouzid YY, Vainberg Y, Masarweh C, Zhou Q, Smilowitz JT, German JB, Mills DA, Lemay DG, Lebrilla CB. 2022. The development of the Davis food glycopedia-A glycan encyclopedia of food. Nutrients 14:1639. https://doi.org/10.3390/nu14081639
32. NRC. 2006. Nutrient requirements of dogs and cats. National Academies Press, Washington, D.C.
33. Brosey BP, Hill RC, Scott KC. 2000. Gastrointestinal volatile fatty acid concentrations and pH in cats. Am J Vet Res 61:359–361. https://doi.org/10.2460/ajvr.2000.61.359
34. Wyse CA, McLellan J, Dickie AM, Sutton DGM, Preston T, Yam PS. 2003. A review of methods for assessment of the rate of gastric emptying in the dog and cat: 1898-2002. J Vet Intern Med 17:609–621. https://doi.org/10.1111/j.1939-1676.2003.tb02491.x
35. Case RM, Harper AA, Scratcherd T. 1969. The secretion of electrolytes and enzymes by the pancreas of the anaesthetized cat. J Physiol 201:335–348. https://doi.org/10.1113/jphysiol.1969.sp008759
36. Kienzle E. 1993. Carbohydrate metabolism of the cat 1. Activity of amylase in the gastrointestinal tract of the cat. Animal Physiology Nutrition 69:92–101. https://doi.org/10.1111/j.1439-0396.1993.tb00793.x
37. Hobson CA, Vigue L, Naimi S, Chassaing B, Magnan M, Bonacorsi S, Gachet B, El Meouche I, Birgy A, Tenaillon O. 2022. MiniBioReactor Array (MBRA) *in vitro* gut model: a reliable system to study microbiota-dependent response to antibiotic treatment. JAC Antimicrob Resist 4:dlac077. https://doi.org/10.1093/jacamr/dlac077
38. Auchtung JM, Robinson CD, Britton RA. 2015. Cultivation of stable, reproducible microbial communities from different fecal donors using minibioreactor arrays (MBRAs). Microbiome 3:42. https://doi.org/10.1186/s40168-015-0106-5
39. Bosch G, Heesen L, de Melo Santos K, Pellikaan WF, Cone JW, Hendriks WH. 2017. Evaluation of an *in vitro* fibre fermentation method using feline faecal inocula: repeatability and reproducibility. J Nutr Sci 6:e25. https://doi.org/10.1017/jns.2017.22
40. Weng C-YC, Suarez C, Cheang SE, Couture G, Goodson ML, Barboza M, Kalanetra KM, Masarweh CF, Mills DA, Raybould HE, Lebrilla CB. 2024. Quantifying gut microbial short-chain fatty acids and their isotopomers in mechanistic studies using a rapid, readily expandable LC-MS platform. Anal Chem 96:2415–2424. https://doi.org/10.1021/acs.analchem.3c04352
41. Lewis ZT, Totten SM, Smilowitz JT, Popovic M, Parker E, Lemay DG, Van Tassell ML, Miller MJ, Jin Y-S, German JB, Lebrilla CB, Mills DA. 2015. Maternal fucosyltransferase 2 status affects the gut bifidobacterial communities of breastfed infants. Microbiome 3:13. https://doi.org/10.1186/s40168-015-0071-z
42. Joshi N. 2011. Sabre: a barcode demultiplexing and trimming tool for FastQ files. GitHub, San Francisco, CA, USA.
43. Bolyen E, Rideout JR, Dillon MR, Bokulich NA, Abnet CC, Al-Ghalith GA, Alexander H, Alm EJ, Arumugam M, Asnicar F, et al. 2019. Reproducible, interactive, scalable and extensible microbiome data science using QIIME 2. Nat Biotechnol 37:852–857. https://doi.org/10.1038/s41587-019-0209-9
44. Callahan BJ, McMurdie PJ, Rosen MJ, Han AW, Johnson AJA, Holmes SP. 2016. DADA2: high-resolution sample inference from Illumina amplicon data. Nat Methods 13:581–583. https://doi.org/10.1038/nmeth.3869
45. Bokulich NA, Kaehler BD, Rideout JR, Dillon M, Bolyen E, Knight R, Huttley GA, Gregory Caporaso J. 2018. Optimizing taxonomic

classification of marker-gene amplicon sequences with QIIME 2's q2-feature-classifier plugin. Microbiome 6:90. https://doi.org/10.1186/s40168-018-0470-z
46. Quast C, Pruesse E, Yilmaz P, Gerken J, Schweer T, Yarza P, Peplies J, Glöckner FO. 2013. The SILVA ribosomal RNA gene database project: improved data processing and web-based tools. Nucleic Acids Res 41:D590–D596. https://doi.org/10.1093/nar/gks1219
47. Robeson MS, O'Rourke DR, Kaehler BD, Ziemski M, Dillon MR, Foster JT, Bokulich NA. 2020. RESCRIPt: reproducible sequence taxonomy reference database management for the masses. bioRxiv. https://doi.org/10.1101/2020.10.05.326504
48. Davis NM, Proctor DM, Holmes SP, Relman DA, Callahan BJ. 2018. Simple statistical identification and removal of contaminant sequences in marker-gene and metagenomics data. Microbiome 6:226. https://doi.org/10.1186/s40168-018-0605-2
49. McMurdie PJ, Holmes S. 2013. phyloseq: an R package for reproducible interactive analysis and graphics of microbiome census data. PLoS One 8:e61217. https://doi.org/10.1371/journal.pone.0061217
50. R Core Team. 2021. R: a language and environment for statistical computing. Computer software. R foundation for statistical computing.
51. Hahsler M, Piekenbrock M, Doran D. 2019. dbscan: fast density-based clustering with R. J Stat Softw 91. https://doi.org/10.18637/jss.v091.i01
52. Schubert E, Sander J, Ester M, Kriegel HP, Xu X. 2017. DBSCAN revisited, revisited. ACM Trans Database Syst 42:1–21. https://doi.org/10.1145/3068335
53. Oksanen J, Kindt R, Legendre P, O'Hara B, Stevens MHH, Oksanen MJ, Suggests M. 2007. The vegan package. Community ecology package 10:719.
54. Kuznetsova A, Brockhoff PB, Christensen RHB. 2017. lmertest package: tests in linear mixed effects models. J Stat Soft 82:1–26. https://doi.org/10.18637/jss.v082.i13
55. Lozupone CA, Hamady M, Kelley ST, Knight R. 2007. Quantitative and qualitative beta diversity measures lead to different insights into factors that structure microbial communities. Appl Environ Microbiol 73:1576–1585. https://doi.org/10.1128/AEM.01996-06
56. Mandal S, Van Treuren W, White RA, Eggesbø M, Knight R, Peddada SD. 2015. Analysis of composition of microbiomes: a novel method for studying microbial composition. Microb Ecol Health Dis 26:27663. https://doi.org/10.3402/mehd.v26.27663
57. Makki K, Deehan EC, Walter J, Bäckhed F. 2018. The impact of dietary fiber on gut microbiota in host health and disease. Cell Host Microbe 23:705–715. https://doi.org/10.1016/j.chom.2018.05.012
58. Rogowski A, Briggs JA, Mortimer JC, Tryfona T, Terrapon N, Lowe EC, Baslé A, Morland C, Day AM, Zheng H, Rogers TE, Thompson P, Hawkins AR, Yadav MP, Henrissat B, Martens EC, Dupree P, Gilbert HJ, Bolam DN. 2015. Glycan complexity dictates microbial resource allocation in the large intestine. Nat Commun 6:7481. https://doi.org/10.1038/ncomms8481
59. Koropatkin NM, Cameron EA, Martens EC. 2012. How glycan metabolism shapes the human gut microbiota. Nat Rev Microbiol 10:323–335. https://doi.org/10.1038/nrmicro2746
60. Cantu-Jungles TM, Bulut N, Chambry E, Ruthes A, Iacomini M, Keshavarzian A, Johnson TA, Hamaker BR. 2021. Dietary fiber hierarchical specificity: the missing link for predictable and strong shifts in gut bacterial communities. mBio 12:e0102821. https://doi.org/10.1128/mBio.01028-21
61. Grabarics M, Lettow M, Kirschbaum C, Greis K, Manz C, Pagel K. 2022. Mass spectrometry-based techniques to elucidate the sugar code. Chem Rev 122:7840–7908. https://doi.org/10.1021/acs.chemrev.1c00380
62. De Filippis F, Pellegrini N, Vannini L, Jeffery IB, La Storia A, Laghi L, Serrazanetti DI, Di Cagno R, Ferrocino I, Lazzi C, Turroni S, Cocolin L, Brigidi P, Neviani E, Gobbetti M, O'Toole PW, Ercolini D. 2016. High-level adherence to a Mediterranean diet beneficially impacts the gut microbiota and associated metabolome. Gut 65:1812–1821. https://doi.org/10.1136/gutjnl-2015-309957
63. Roager HM, Vogt JK, Kristensen M, Hansen LBS, Ibrügger S, Mærkedahl RB, Bahl MI, Lind MV, Nielsen RL, Frøkiær H, et al. 2019. Whole grain-rich diet reduces body weight and systemic low-grade inflammation without inducing major changes of the gut microbiome: a randomised cross-over trial. Gut 68:83–93. https://doi.org/10.1136/gutjnl-2017-314786
64. El Kaoutari A, Armougom F, Gordon JI, Raoult D, Henrissat B. 2013. The abundance and variety of carbohydrate-active enzymes in the human gut microbiota. Nat Rev Microbiol 11:497–504. https://doi.org/10.1038/nrmicro3050
65. Wardman JF, Bains RK, Rahfeld P, Withers SG. 2022. Carbohydrate-active enzymes (CAZymes) in the gut microbiome. Nat Rev Microbiol 20:542–556. https://doi.org/10.1038/s41579-022-00712-1
66. Coker JK, Moyne O, Rodionov DA, Zengler K. 2021. Carbohydrates great and small, from dietary fiber to sialic acids: how glycans influence the gut microbiome and affect human health. Gut Microbes 13:1–18. https://doi.org/10.1080/19490976.2020.1869502
67. Ravcheev DA, Thiele I. 2017. Comparative genomic analysis of the human gut microbiome reveals a broad distribution of metabolic pathways for the degradation of host-synthetized mucin glycans and utilization of mucin-derived monosaccharides. Front Genet 8:111. https://doi.org/10.3389/fgene.2017.00111
68. Mendis M, Martens EC, Simsek S. 2018. How fine structural differences of xylooligosaccharides and arabinoxylooligosaccharides regulate differential growth of bacteroides species. J Agric Food Chem 66:8398–8405. https://doi.org/10.1021/acs.jafc.8b01263
69. Gálvez EJC, Iljazovic A, Amend L, Lesker TR, Renault T, Thiemann S, Hao L, Roy U, Gronow A, Charpentier E, Strowig T. 2020. Distinct polysaccharide utilization determines interspecies competition between intestinal *Prevotella* spp. Cell Host Microbe 28:838–852. https://doi.org/10.1016/j.chom.2020.09.012
70. Lancaster SM, Lee-McMullen B, Abbott CW, Quijada JV, Hornburg D, Park H, Perelman D, Peterson DJ, Tang M, Robinson A, Ahadi S, Contrepois K, Hung C-J, Ashland M, McLaughlin T, Boonyanit A, Horning A, Sonnenburg JL, Snyder MP. 2022. Global, distinctive, and personal changes in molecular and microbial profiles by specific fibers in humans. Cell Host Microbe 30:848–862. https://doi.org/10.1016/j.chom.2022.03.036
71. Yasuma T, Toda M, Abdel-Hamid AM, D'Alessandro-Gabazza C, Kobayashi T, Nishihama K, D'Alessandro VF, Pereira GV, Mackie RI, Gabazza EC, Cann I. 2021. Degradation products of complex arabinoxylans by *Bacteroides intestinalis* enhance the host immune response. Microorganisms 9:1126. https://doi.org/10.3390/microorganisms9061126
72. Lin C-Y, Jha AR, Oba PM, Yotis SM, Shmalberg J, Honaker RW, Swanson KS. 2022. Longitudinal fecal microbiome and metabolite data demonstrate rapid shifts and subsequent stabilization after an abrupt dietary change in healthy adult dogs. Anim Microbiome 4:46. https://doi.org/10.1186/s42523-022-00194-9
73. Park S-Y, Rao C, Coyte KZ, Kuziel GA, Zhang Y, Huang W, Franzosa EA, Weng J-K, Huttenhower C, Rakoff-Nahoum S. 2022. Strain-level fitness in the gut microbiome is an emergent property of glycans and a single metabolite. Cell 185:513–529. https://doi.org/10.1016/j.cell.2022.01.002
74. Fukuda S, Toh H, Hase K, Oshima K, Nakanishi Y, Yoshimura K, Tobe T, Clarke JM, Topping DL, Suzuki T, Taylor TD, Itoh K, Kikuchi J, Morita H, Hattori M, Ohno H. 2011. Bifidobacteria can protect from enteropathogenic infection through production of acetate. Nature 469:543–547. https://doi.org/10.1038/nature09646
75. Nguyen NK, Deehan EC, Zhang Z, Jin M, Baskota N, Perez-Muñoz ME, Cole J, Tuncil YE, Seethaler B, Wang T, Laville M, Delzenne NM, Bischoff SC, Hamaker BR, Martínez I, Knights D, Bakal JA, Prado CM, Walter J. 2020. Gut microbiota modulation with long-chain corn bran arabinoxylan in adults with overweight and obesity is linked to an individualized temporal increase in fecal propionate. Microbiome 8:118. https://doi.org/10.1186/s40168-020-00887-w
76. Jacobson A, Lam L, Rajendram M, Tamburini F, Honeycutt J, Pham T, Van Treuren W, Pruss K, Stabler SR, Lugo K, Bouley DM, Vilches-Moure JG, Smith M, Sonnenburg JL, Bhatt AS, Huang KC, Monack D. 2018. A gut commensal-produced metabolite mediates colonization resistance to *Salmonella* infection. Cell Host Microbe 24:296–307. https://doi.org/10.1016/j.chom.2018.07.002
77. Louis P, Scott KP, Duncan SH, Flint HJ. 2007. Understanding the effects of diet on bacterial metabolism in the large intestine. J Appl Microbiol 102:1197–1208. https://doi.org/10.1111/j.1365-2672.2007.03322.x

78. Venkatesh M, Mukherjee S, Wang H, Li H, Sun K, Benechet AP, Qiu Z, Maher L, Redinbo MR, Phillips RS, Fleet JC, Kortagere S, Mukherjee P, Fasano A, Le Ven J, Nicholson JK, Dumas ME, Khanna KM, Mani S. 2014. Symbiotic bacterial metabolites regulate gastrointestinal barrier function via the xenobiotic sensor PXR and Toll-like receptor 4. Immunity 41:296–310. https://doi.org/10.1016/j.immuni.2014.06.014
79. Krishnan S, Ding Y, Saedi N, Choi M, Sridharan GV, Sherr DH, Yarmush ML, Alaniz RC, Jayaraman A, Lee K. 2018. Gut microbiota-derived tryptophan metabolites modulate inflammatory response in hepatocytes and macrophages. Cell Rep 23:1099–1111. https://doi.org/10.1016/j.celrep.2018.03.109
80. Flint HJ, Duncan SH, Louis P. 2017. The impact of nutrition on intestinal bacterial communities. Curr Opin Microbiol 38:59–65. https://doi.org/10.1016/j.mib.2017.04.005
81. Lindstad LJ, Lo G, Leivers S, Lu Z, Michalak L, Pereira GV, Røhr ÅK, Martens EC, McKee LS, Louis P, Duncan SH, Westereng B, Pope PB, La Rosa SL. 2021. Human gut *Faecalibacterium prausnitzii* deploys a highly efficient conserved system to cross-feed on β-mannan-derived oligosaccharides. mBio 12:e0362820. https://doi.org/10.1128/mBio.03628-20
82. Bilen M, Cadoret F, Richez M, Tomei E, Daoud Z, Raoult D, Fournier PE. 2018. *Libanicoccus massiliensis* gen. nov., sp. nov., a new bacterium isolated from human stool. New Microbes New Infect 21:63–71. https://doi.org/10.1016/j.nmni.2017.11.001
83. Ndongo S, Lagier JC, Fournier PE, Raoult D, Khelaifia S. 2016. "*Phocea massiliensis*" a new bacterial species isolated from the human gut. New Microbes New Infect 13:67–68. https://doi.org/10.1016/j.nmni.2016.06.009
84. David LA, Maurice CF, Carmody RN, Gootenberg DB, Button JE, Wolfe BE, Ling AV, Devlin AS, Varma Y, Fischbach MA, Biddinger SB, Dutton RJ, Turnbaugh PJ. 2014. Diet rapidly and reproducibly alters the human gut microbiome. Nature 505:559–563. https://doi.org/10.1038/nature12820
85. Parker BJ, Wearsch PA, Veloo ACM, Rodriguez-Palacios A. 2020. The genus alistipes: gut bacteria with emerging implications to inflammation, cancer, and mental health. Front Immunol 11:906. https://doi.org/10.3389/fimmu.2020.00906
86. Marcobal A, Barboza M, Sonnenburg ED, Pudlo N, Martens EC, Desai P, Lebrilla CB, Weimer BC, Mills DA, German JB, Sonnenburg JL. 2011. Bacteroides in the infant gut consume milk oligosaccharides via mucus-utilization pathways. Cell Host Microbe 10:507–514. https://doi.org/10.1016/j.chom.2011.10.007
87. Crouch LI, Liberato MV, Urbanowicz PA, Baslé A, Lamb CA, Stewart CJ, Cooke K, Doona M, Needham S, Brady RR, Berrington JE, Madunic K, Wuhrer M, Chater P, Pearson JP, Glowacki R, Martens EC, Zhang F, Linhardt RJ, Spencer DIR, Bolam DN. 2020. Prominent members of the human gut microbiota express endo-acting O-glycanases to initiate mucin breakdown. Nat Commun 11:4017. https://doi.org/10.1038/s41467-020-17847-5
88. Bell A, Juge N. 2021. Mucosal glycan degradation of the host by the gut microbiota. Glycobiology 31:691–696. https://doi.org/10.1093/glycob/cwaa097
89. Yun EJ, Yu S, Park NJ, Cho Y, Han NR, Jin Y-S, Kim KH. 2021. Metabolic and enzymatic elucidation of cooperative degradation of red seaweed agarose by two human gut bacteria. Sci Rep 11:13955. https://doi.org/10.1038/s41598-021-92872-y
90. La Rosa SL, Kachrimanidou V, Buffetto F, Pope PB, Pudlo NA, Martens EC, Rastall RA, Gibson GR, Westereng B. 2019. Wood-derived dietary fibers promote beneficial human gut microbiota. mSphere 4:e00554-18. https://doi.org/10.1128/mSphere.00554-18
91. Klassen L, Xing X, Tingley JP, Low KE, King ML, Reintjes G, Abbott DW. 2021. Approaches to investigate selective dietary polysaccharide utilization by human gut microbiota at a functional level. Front Microbiol 12:632684. https://doi.org/10.3389/fmicb.2021.632684
92. Galermo AG, Nandita E, Castillo JJ, Amicucci MJ, Lebrilla CB. 2019. Development of an extensive linkage library for characterization of carbohydrates. Anal Chem 91:13022–13031. https://doi.org/10.1021/acs.analchem.9b03101
93. Luis AS, Baslé A, Byrne DP, Wright GSA, London JA, Jin C, Karlsson NG, Hansson GC, Eyers PA, Czjzek M, Barbeyron T, Yates EA, Martens EC, Cartmell A. 2022. Sulfated glycan recognition by carbohydrate sulfatases of the human gut microbiota. Nat Chem Biol 18:841–849. https://doi.org/10.1038/s41589-022-01039-x
94. Luis AS, Briggs J, Zhang X, Farnell B, Ndeh D, Labourel A, Baslé A, Cartmell A, Terrapon N, Stott K, Lowe EC, McLean R, Shearer K, Schückel J, Venditto I, Ralet M-C, Henrissat B, Martens EC, Mosimann SC, Abbott DW, Gilbert HJ. 2018. Dietary pectic glycans are degraded by coordinated enzyme pathways in human colonic *Bacteroides*. Nat Microbiol 3:210–219. https://doi.org/10.1038/s41564-017-0079-1
95. Delannoy-Bruno O, Desai C, Castillo JJ, Couture G, Barve RA, Lombard V, Henrissat B, Cheng J, Han N, Hayashi DK, Meynier A, Vinoy S, Lebrilla CB, Marion S, Heath AC, Barratt MJ, Gordon JI. 2022. An approach for evaluating the effects of dietary fiber polysaccharides on the human gut microbiome and plasma proteome. Proc Natl Acad Sci U S A 119:e2123411119. https://doi.org/10.1073/pnas.2123411119
96. Amicucci MJ, Nandita E, Galermo AG, Castillo JJ, Chen S, Park D, Smilowitz JT, German JB, Mills DA, Lebrilla CB. 2020. A nonenzymatic method for cleaving polysaccharides to yield oligosaccharides for structural analysis. Nat Commun 11:3963. https://doi.org/10.1038/s41467-020-17778-1
97. Bojar D, Powers RK, Camacho DM, Collins JJ. 2021. Deep-learning resources for studying glycan-mediated host-microbe interactions. Cell Host Microbe 29:132–144. https://doi.org/10.1016/j.chom.2020.10.004
98. Barratt MJ, Lebrilla C, Shapiro H-Y, Gordon JI. 2017. The gut microbiota, food science, and human nutrition: a timely marriage. Cell Host Microbe 22:134–141. https://doi.org/10.1016/j.chom.2017.07.006
99. Delannoy-Bruno O, Desai C, Raman AS, Chen RY, Hibberd MC, Cheng J, Han N, Castillo JJ, Couture G, Lebrilla CB, Barve RA, Lombard V, Henrissat B, Leyn SA, Rodionov DA, Osterman AL, Hayashi DK, Meynier A, Vinoy S, Kirbach K, Wilmot T, Heath AC, Klein S, Barratt MJ, Gordon JI. 2021. Evaluating microbiome-directed fibre snacks in gnotobiotic mice and humans. Nature 595:91–95. https://doi.org/10.1038/s41586-021-03671-4
100. Holmes ZC, Villa MM, Durand HK, Jiang S, Dallow EP, Petrone BL, Silverman JD, Lin P-H, David LA. 2022. Microbiota responses to different prebiotics are conserved within individuals and associated with habitual fiber intake. Microbiome 10:114. https://doi.org/10.1186/s40168-022-01307-x